A Network-Theoretical Perspective on Oscillator-Based Ising Machines

Bakr Al Beattie[1] and Karlheinz Ochs[1]

[1]Ruhr-Universitat Bochum Fakultat fur Elektrotechnik und Informationstechnik

October 13, 2022

Abstract

The standard van Neumann computer excels at many things. However, it can be very inefficient in solving optimization problems with a large solution space. For that reason, a novel analog approach, the oscillator-based Ising machine, has been proposed as a better alternative for dealing with such problems. In this work, we review the concept of oscillator-based Ising machines. In particular, we address how optimization problems can be mapped onto such machines when the QUBO formulation is given. Furthermore, we provide an ideal circuit that can be used in combination with the wave digital concept for real-time simulated annealing. The functionality of this circuit is explained on the basis of a Lyapunov stability analysis. The latter also provides an answer for the question: when has the Ising machine solved a mapped problem? At the end, we provide emulation results demonstrating the correlation between functionality and stability of the discussed machine. These results show that mapping a problem onto an Ising machine effectively maps the solution of the problem onto an equilibrium of the phase space.

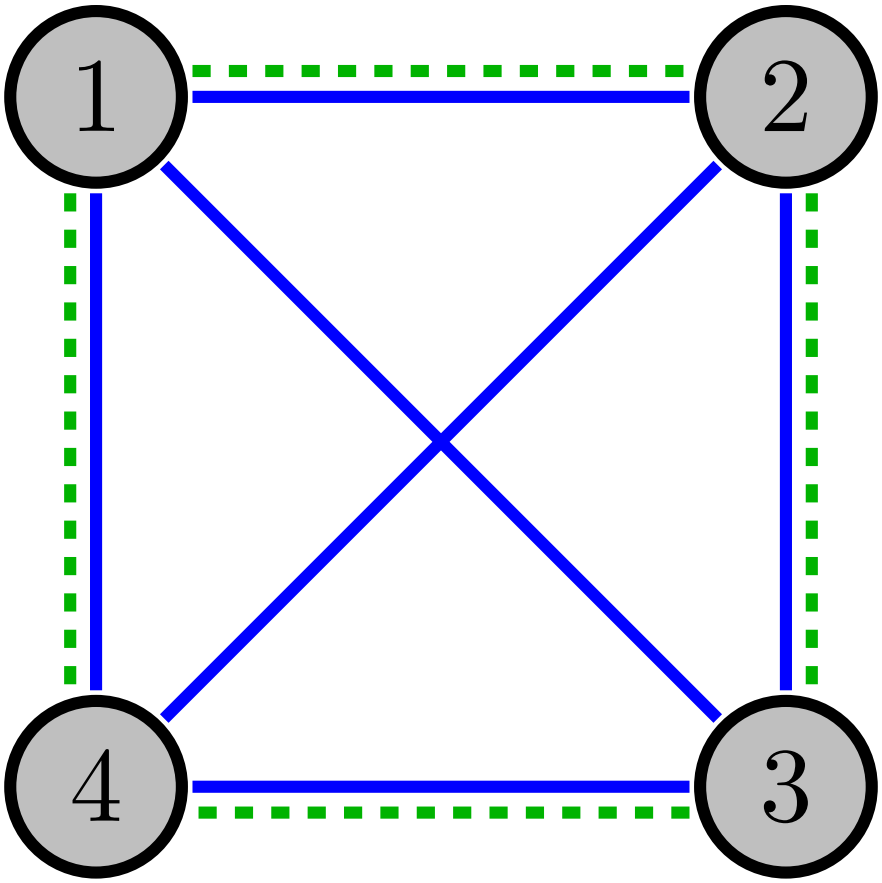

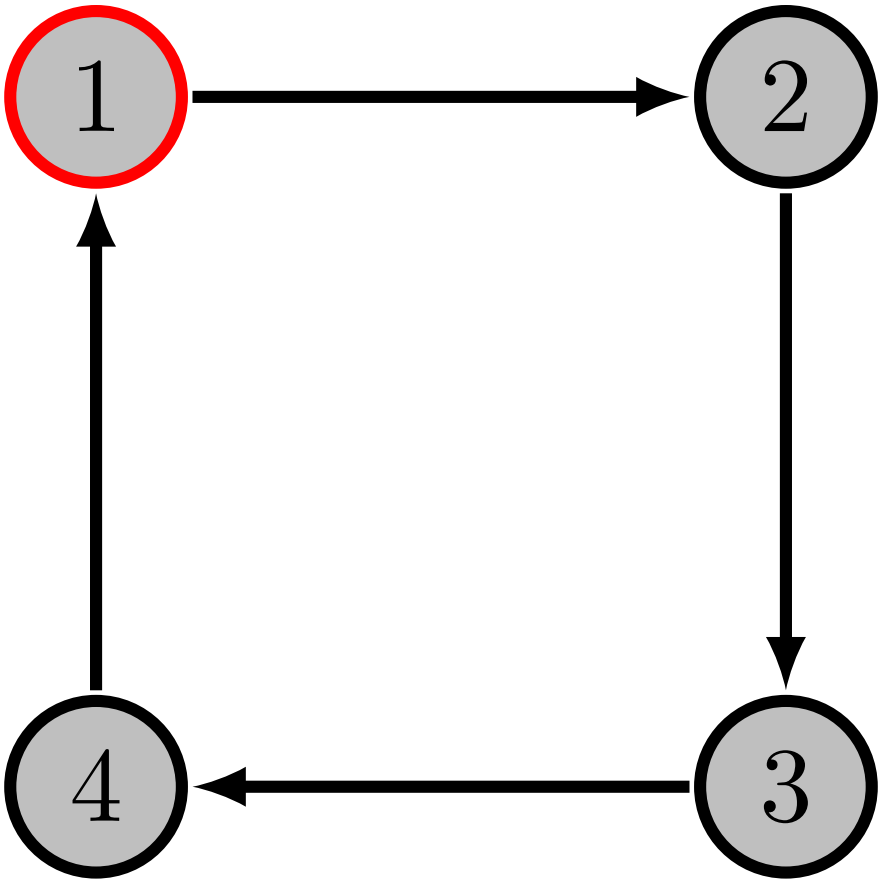

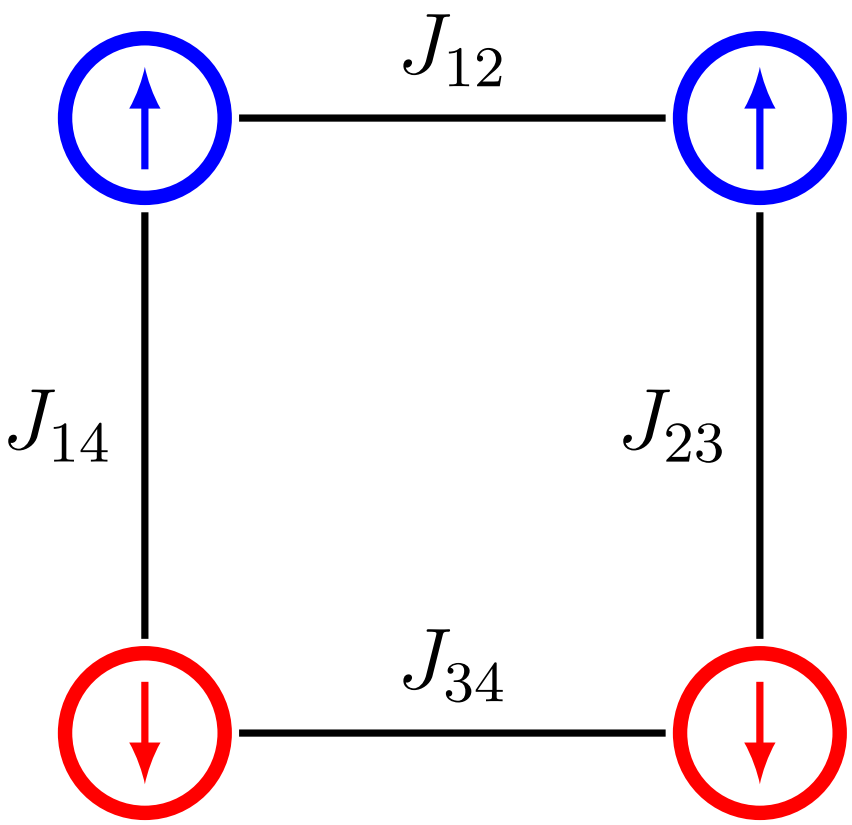

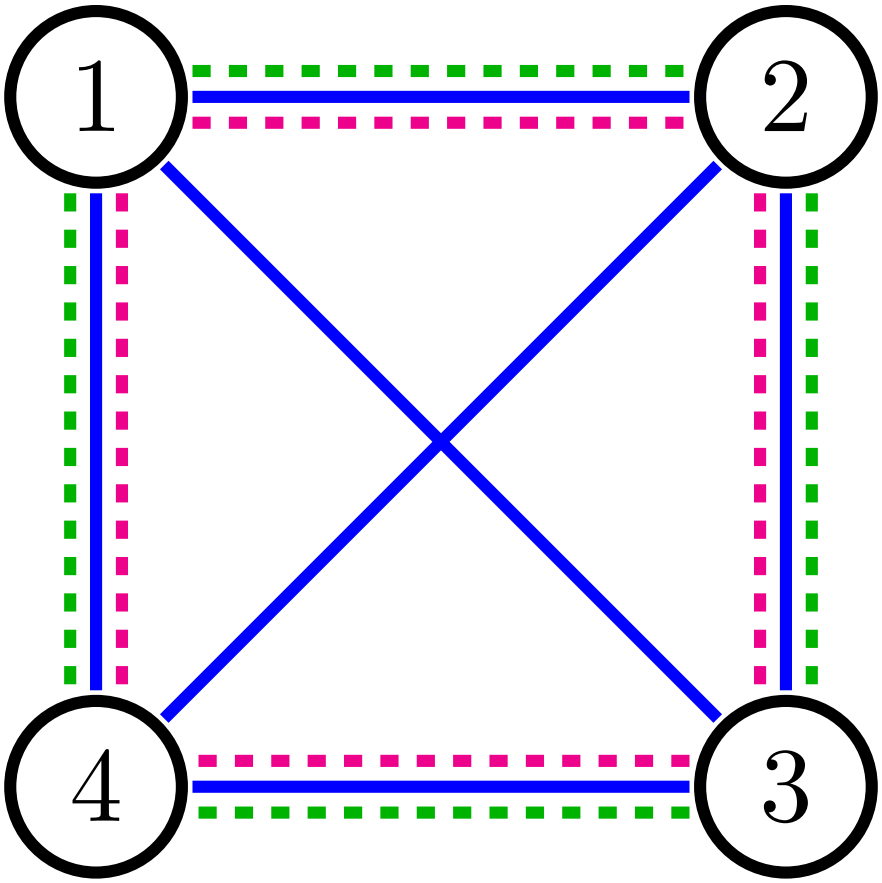

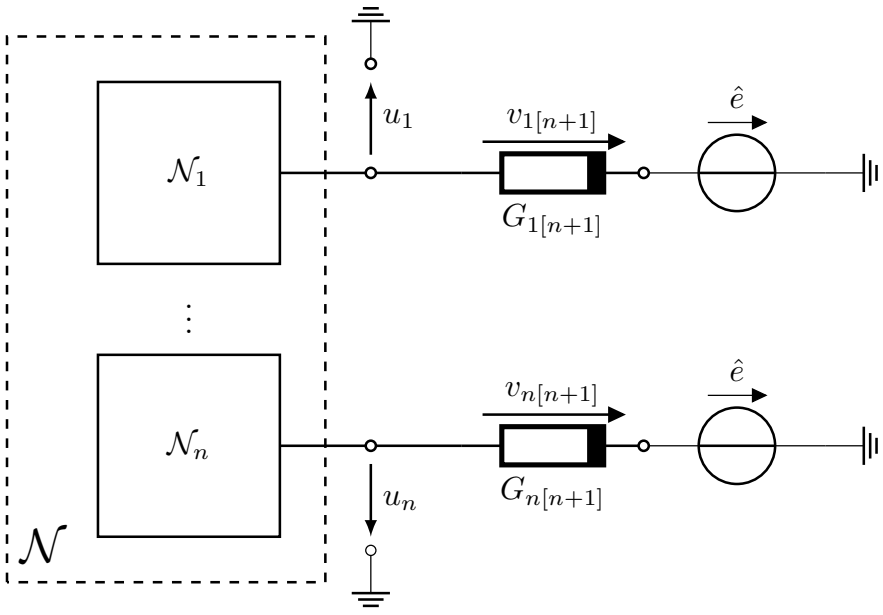

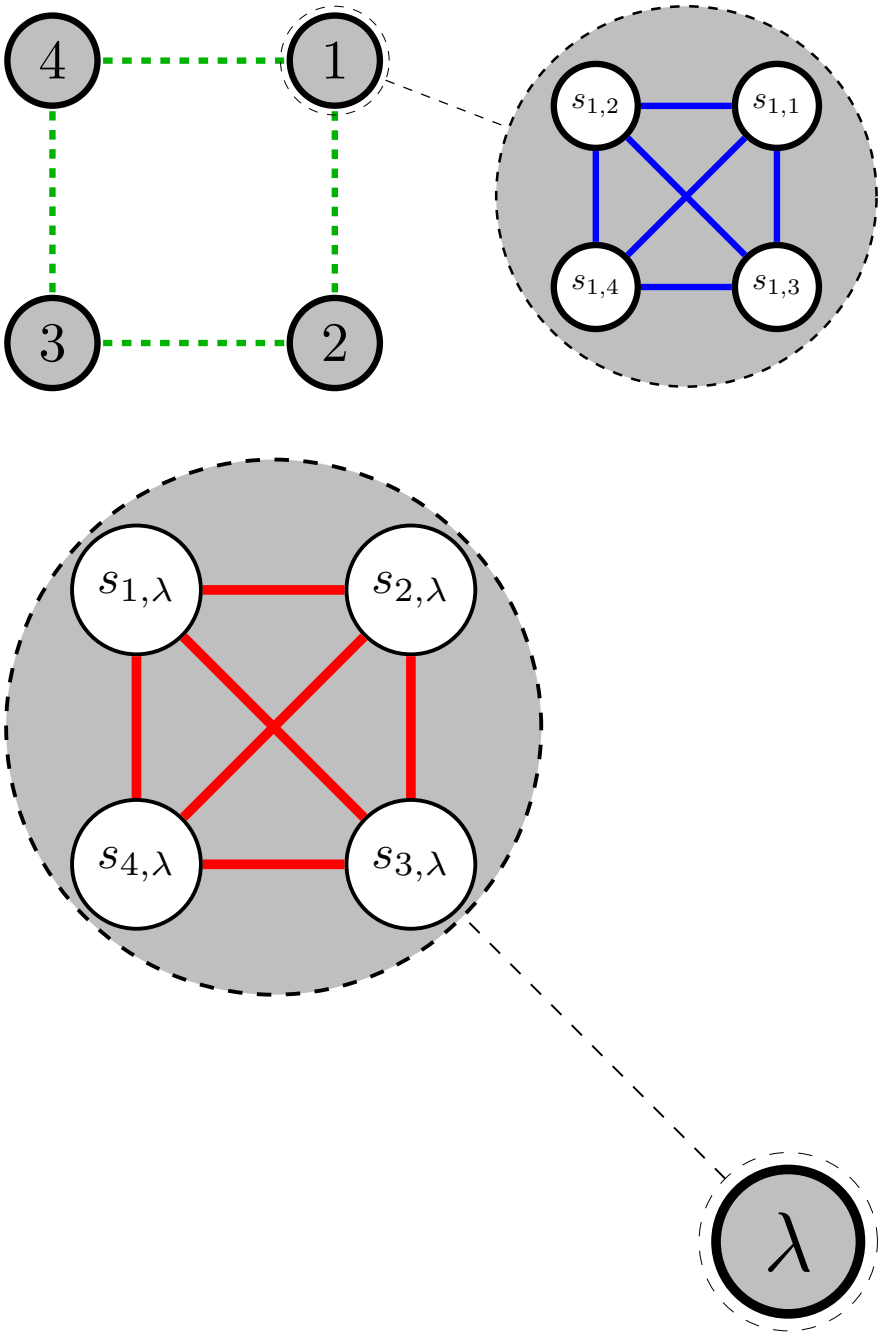

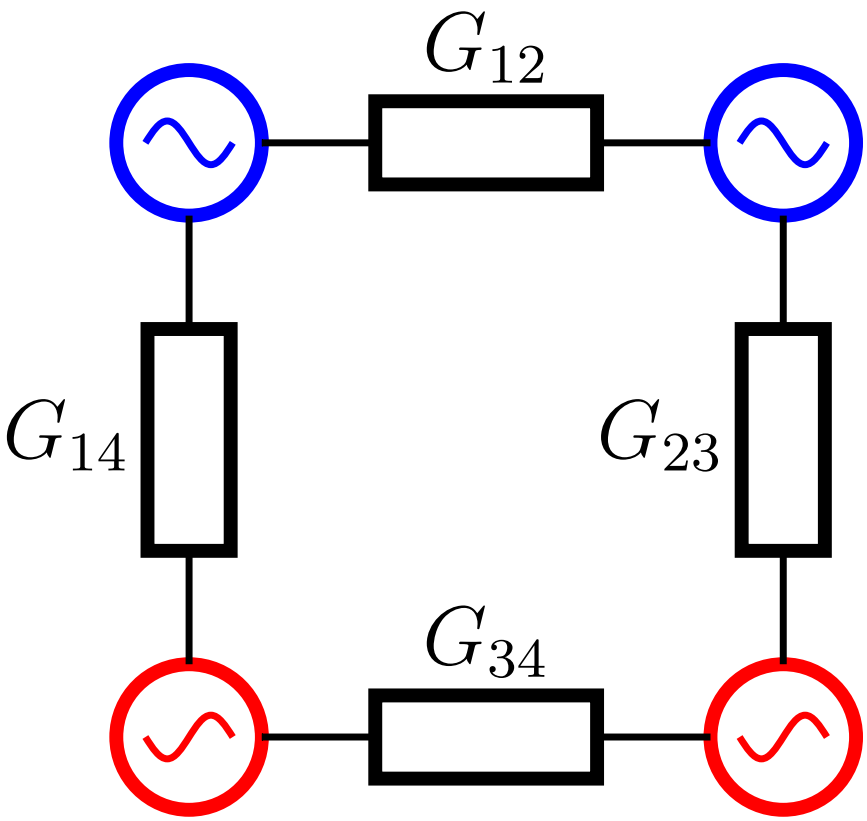

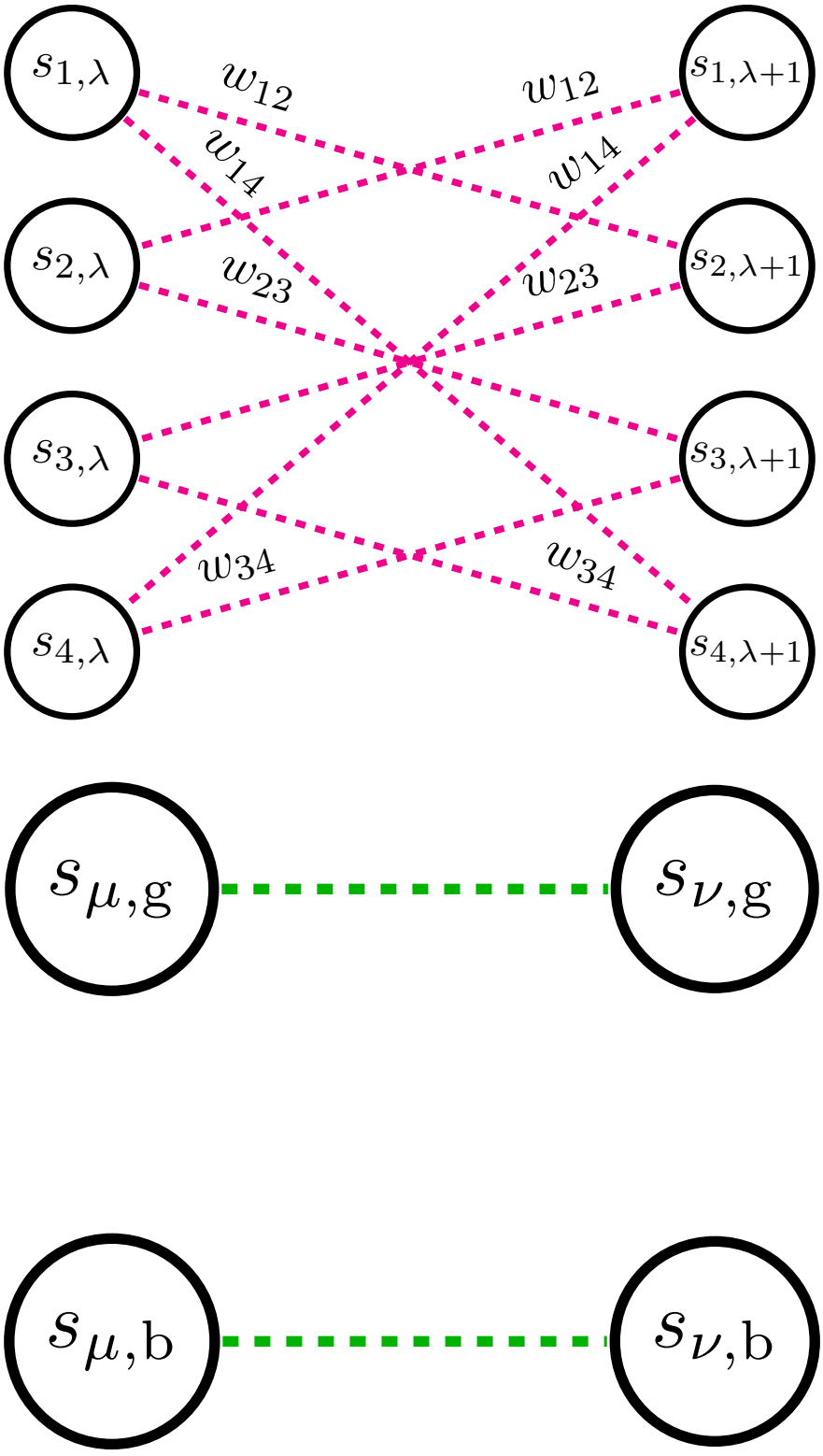

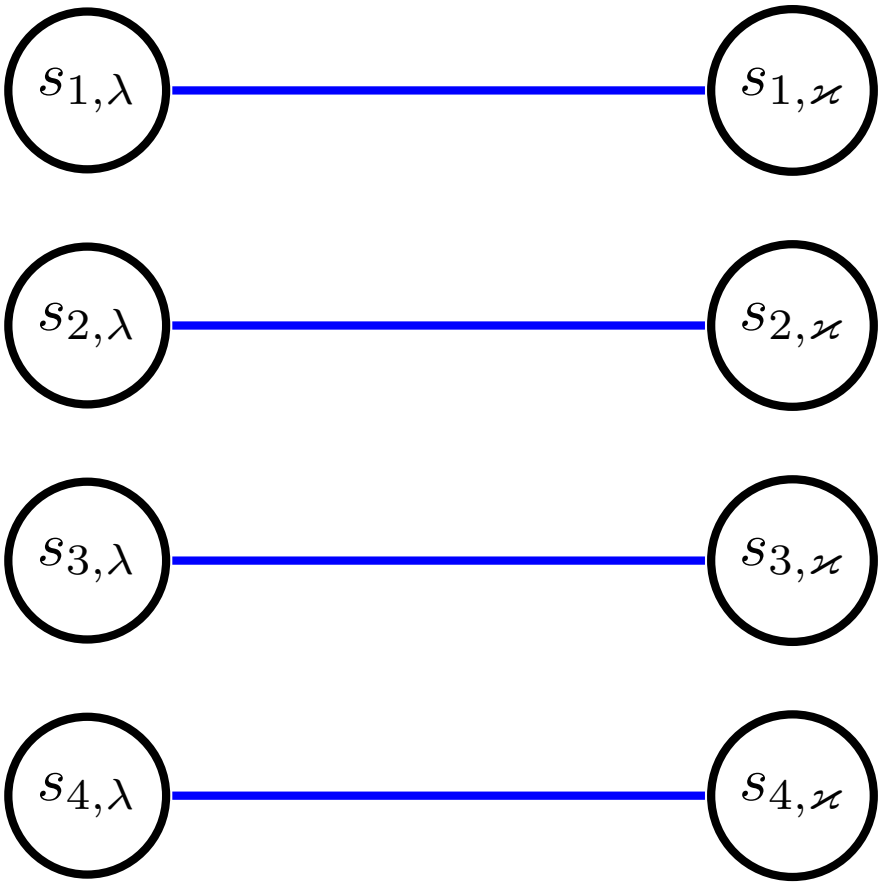

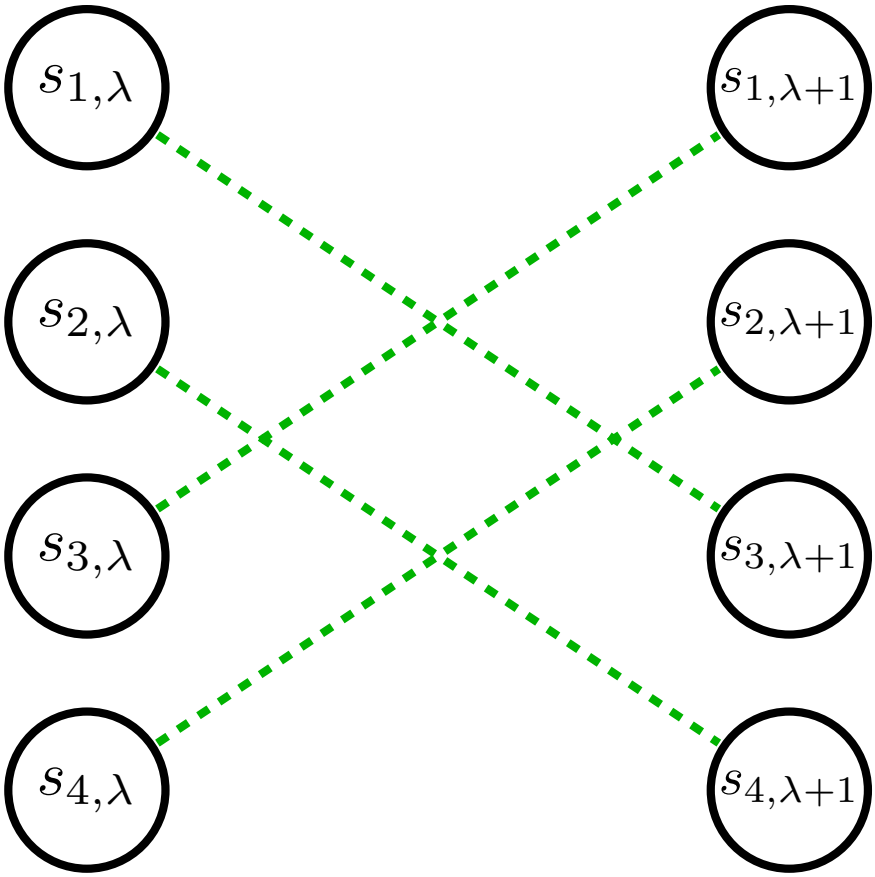

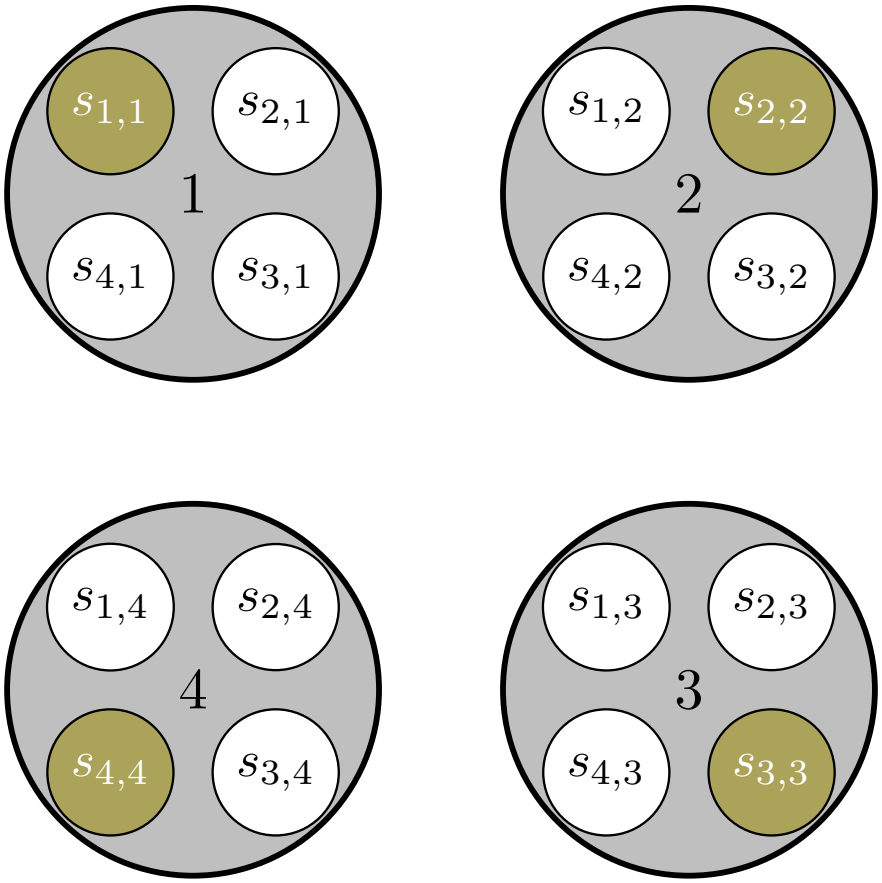

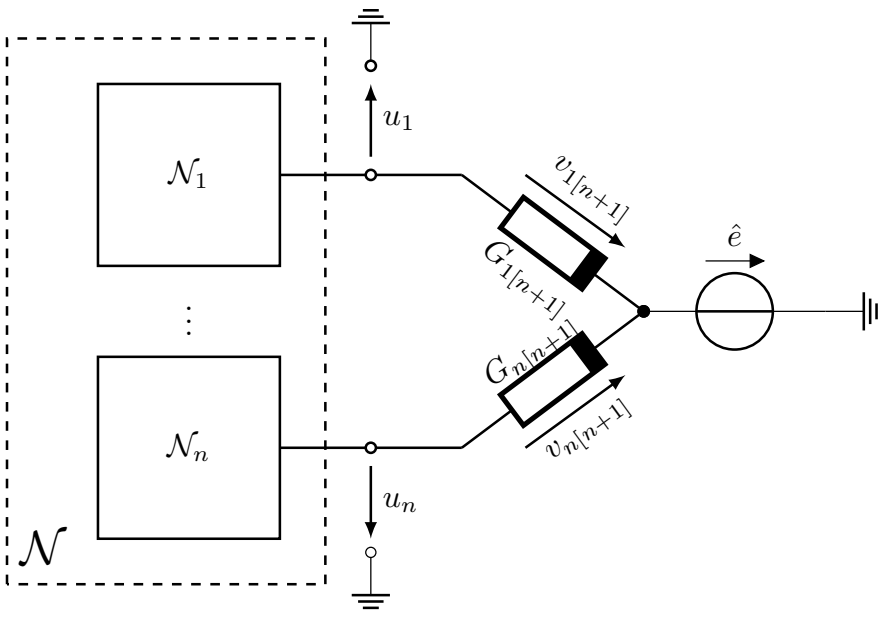

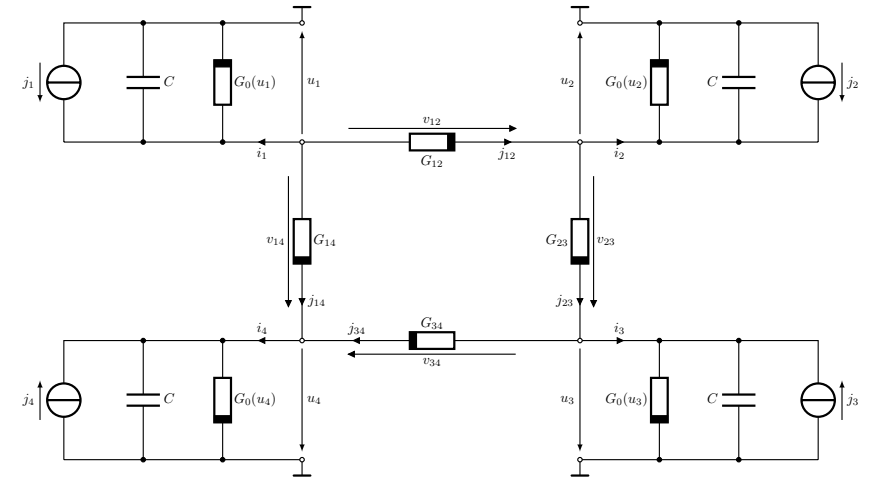

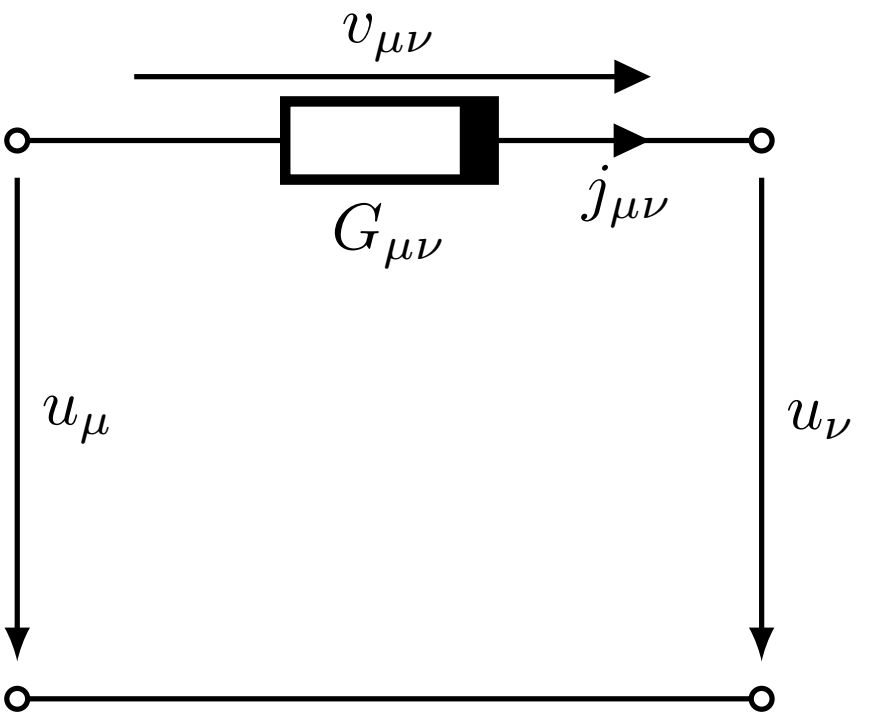

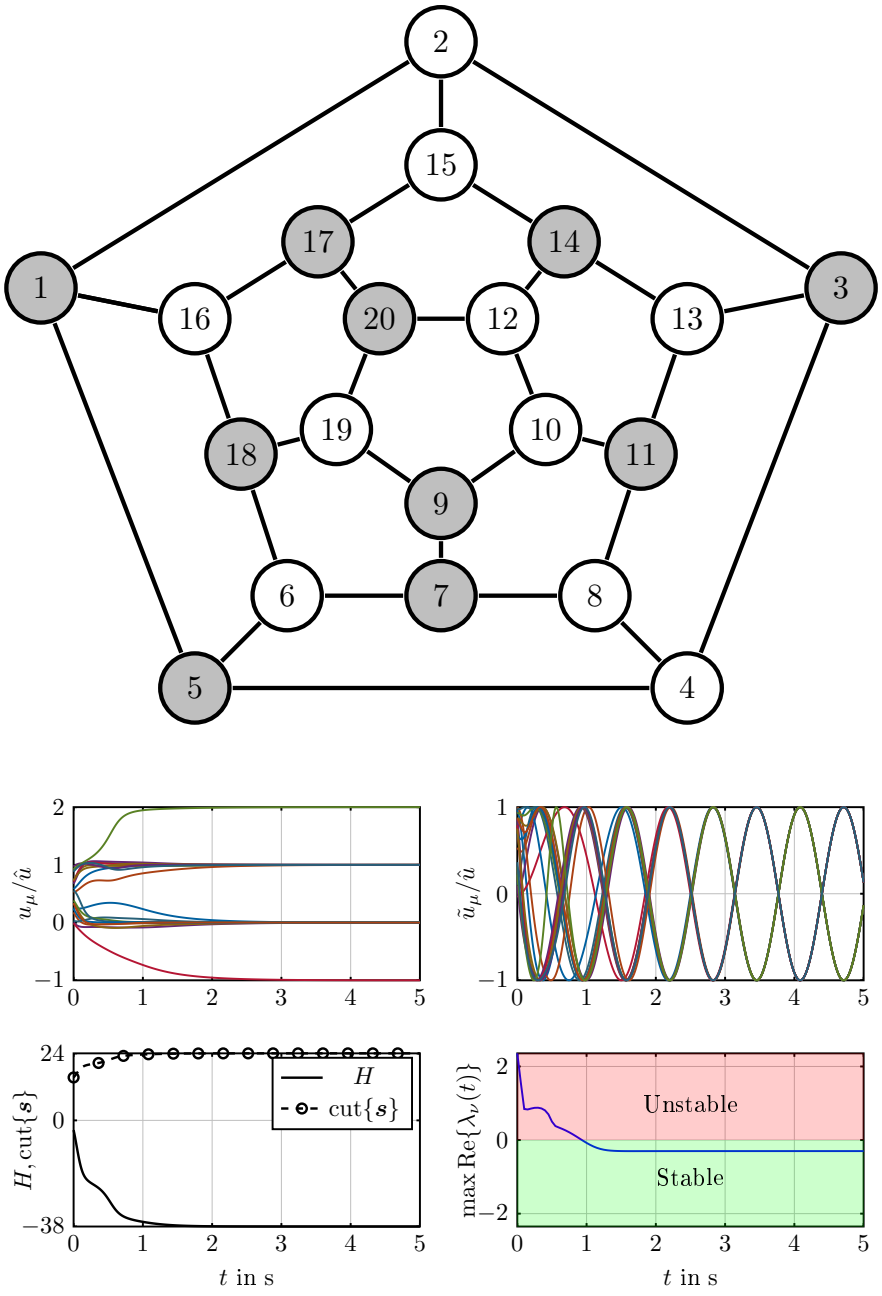

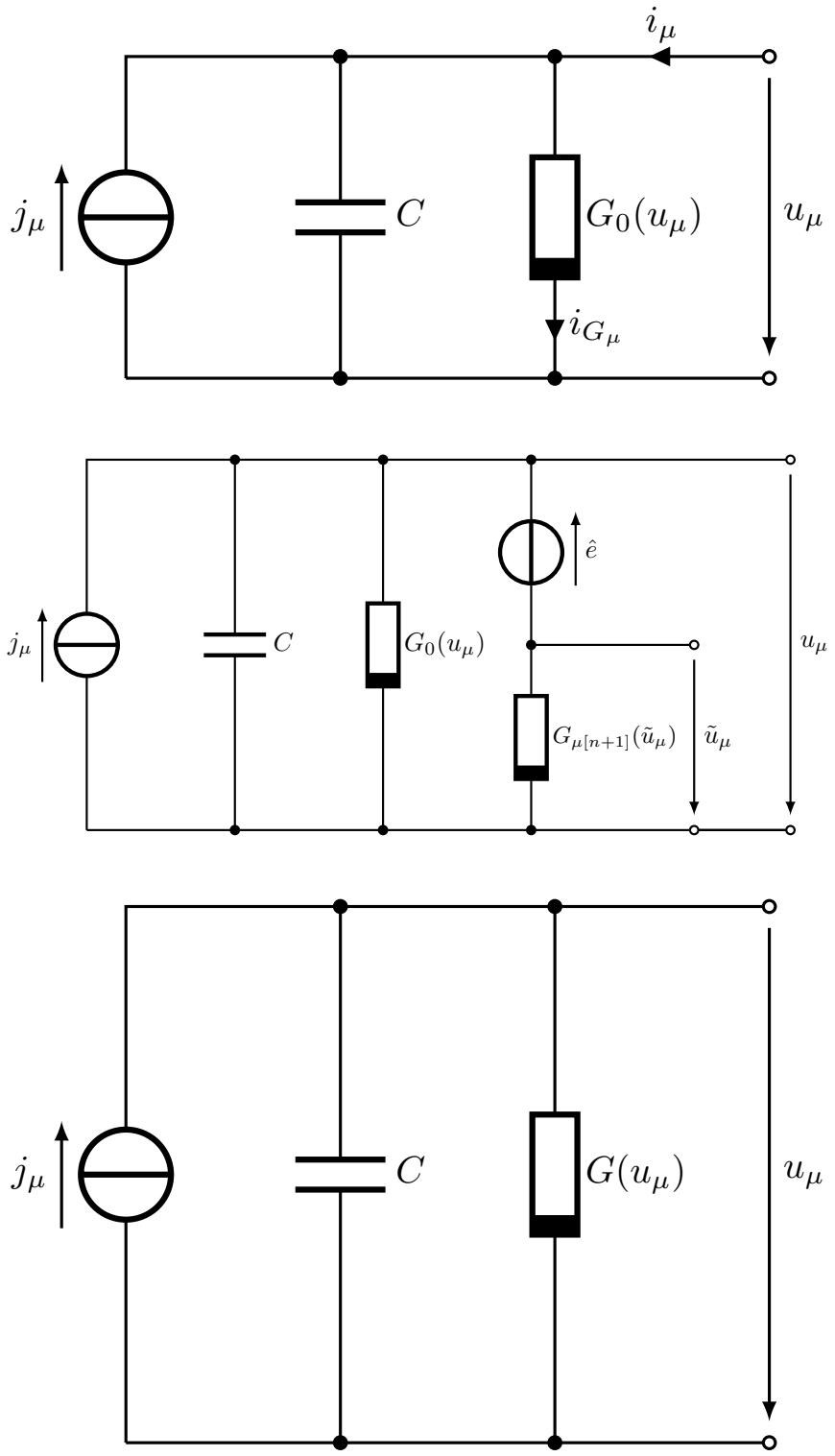

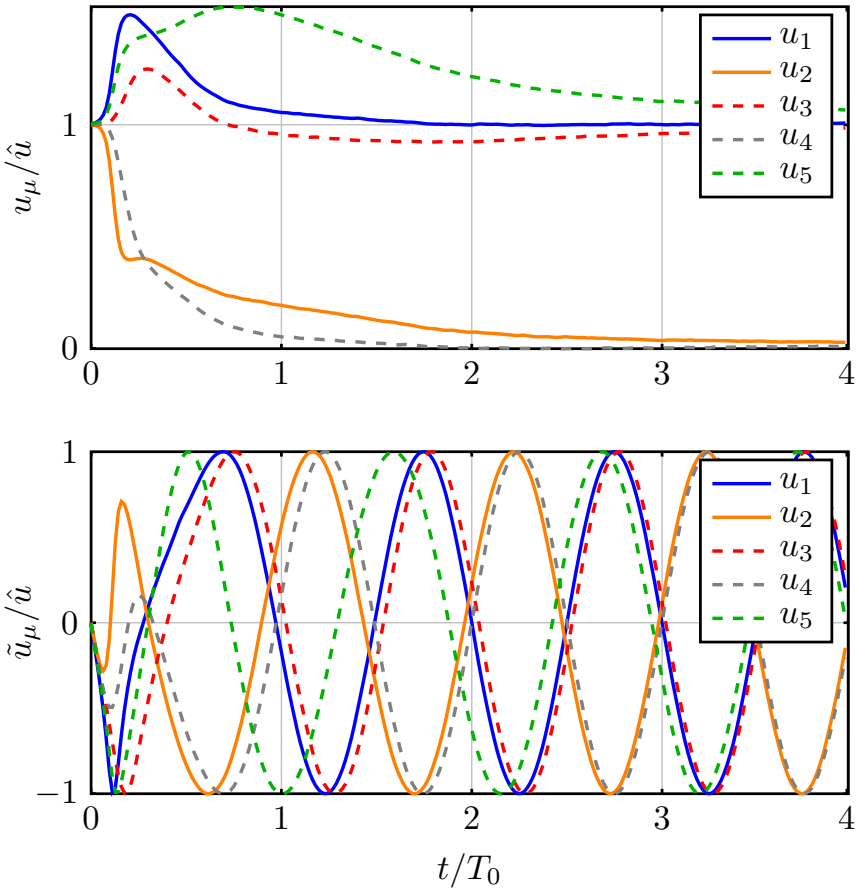

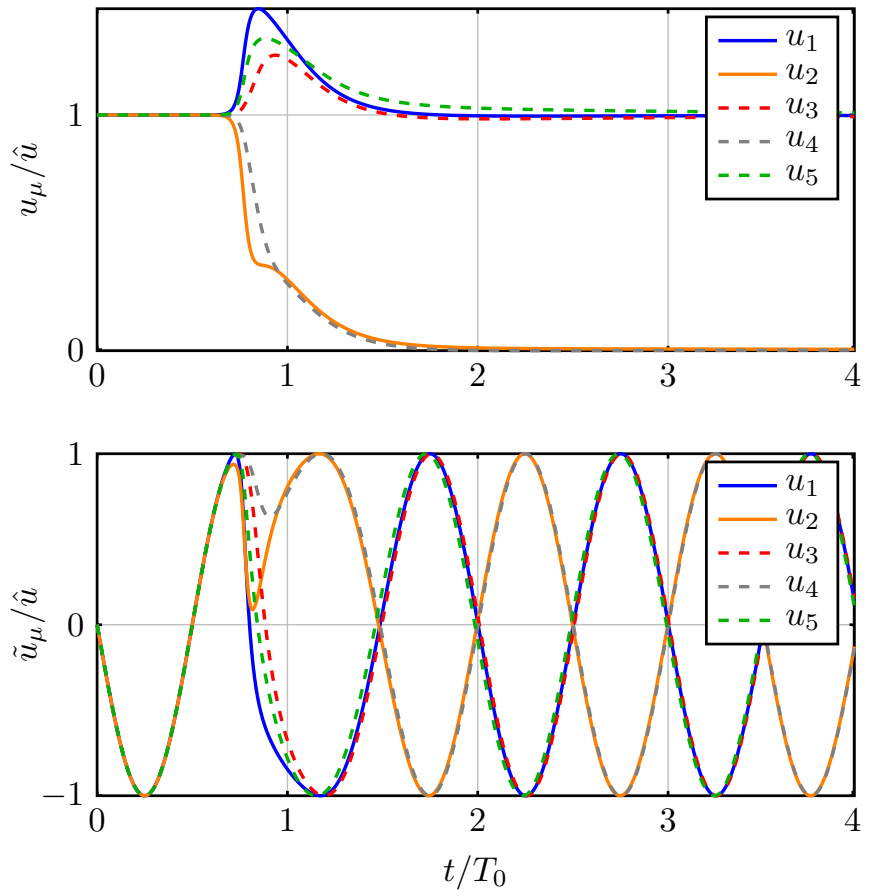

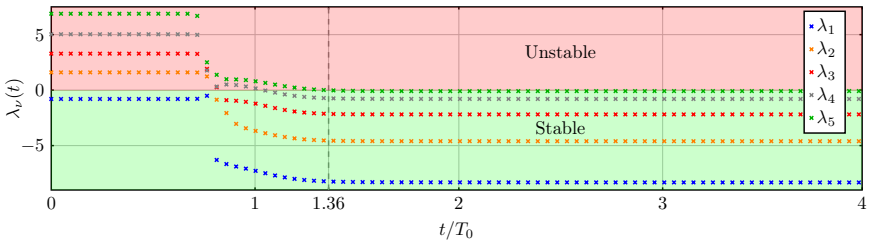

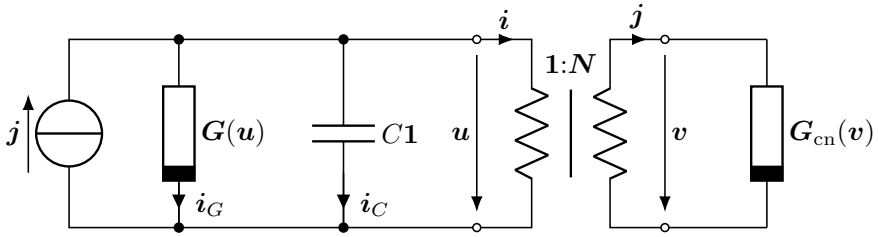

Received: Added at production | Revised: Added at production | Accepted: Added at production

DOI: xxx/xxxx

ORIGINAL PAPER

A Network-Theoretical Perspective on Oscillator-Based Ising Machines†

Bakr Al Beattie | Karlheinz Ochs

Chair of digital communication systems, Faculty of electrical engineering and information technology, Ruhr-University Bochum, 44801 Bochum, Germany

Correspondence
Bakr Al Beattie, Chair of digital communication systems, Faculty of electrical engineering and information technology, Ruhr-University Bochum, 44801 Bochum, Germany
Email: bakr.albeattie@rub.de

Funding Information
This research was supported by the Deutsche Forschungsgemeinschaft (DFG) – Project-ID 434434223 – SFB 1461

Summary

The standard van Neumann computer excels at many things. However, it can be very inefficient in solving optimization problems with a large solution space. For that reason, a novel analog approach, the oscillator-based Ising machine, has been proposed as a better alternative for dealing with such problems. In this work, we review the concept of oscillator-based Ising machines. In particular, we address how optimization problems can be mapped onto such machines when the QUBO formulation is given. Furthermore, we provide an ideal circuit that can be used in combination with the wave digital concept for real-time simulated annealing. The functionality of this circuit is explained on the basis of a Lyapunov stability analysis. The latter also provides an answer for the question: when has the Ising machine solved a mapped problem? At the end, we provide emulation results demonstrating the correlation between functionality and stability of the discussed machine. These results show that mapping a problem onto an Ising machine effectively maps the solution of the problem onto an equilibrium of the phase space.

KEYWORDS:
Ising machine, unconventional computing, Kuramoto model, Lyapunov stability

1 | INTRODUCTION

As the progress in van-Neumann-based technology begins to stagnate, scientific research is slowly gravitating towards finding alternative technologies that can supplement the deficiencies of standard computers[1,2]. In this context, oscillator-based Ising machines are a promising approach for solving combinatorial optimization problems with a large solution space[3]. Their hardware implementation is commonly based on a network of diffusively coupled (nonlinear) oscillators[4,5,6,7,8]. Although in recent years, we have also seen a number of optical implementations, so-called coherent Ising machines[9,10,11,12].

In principle, all Ising machines are built, such that they have the natural tendency to minimize a scalar function, the so-called Ising Hamiltonian, which relates to the Ising model[13] and describes the energy of a lattice consisting of magnetically coupled spins,

$$H = -\boldsymbol{s}^{\mathrm{T}}\boldsymbol{J}\boldsymbol{s} - \boldsymbol{h}^{\mathrm{T}}\boldsymbol{s}\,, \quad \boldsymbol{J} = \boldsymbol{J}^{\mathrm{T}}\,, \quad \boldsymbol{e}_{\nu}^{\mathrm{T}}\boldsymbol{s} = s_{\nu} \in \{\pm 1\}\,, \tag{1}$$

where $\boldsymbol{e}_{\mu}$ denotes a unit vector with a one in the μ-th entry. The vector of spin variables $\boldsymbol{s}$ has the entries s_{ν} describing the orientation of the ν-th spin in the lattice. In general, these spins can either point upwards $s_{\nu} = 1$ or downwards $s_{\nu} = -1$. The mutual coupling is described by the coupling coefficient matrix $\boldsymbol{J}$, whose $\mu\nu$-th element, $J_{\mu\nu}$, describes the magnetic coupling between the μ-th and ν-th spin in the lattice. Moreover, the vector $\boldsymbol{h}$ is the external coupling vector, whose ν-th entry describes

†Bakr Al Beattie and Karlheinz Ochs should be considered joint first author

an external coupling between the ν-th spin and an external magnetic field. In the following, we refer to the corresponding term as the Zeeman term.

To solve a combinatorial optimization problem, one must map the considered problem onto the Ising Hamiltonian. In the past decade, many optimization problems (including Karp's 21 NP-problems) have been successfully mapped onto the Ising Hamiltonian [14,15,16,17,18,19,20]. Here, mapping refers to the procedure of formulating a Hamiltonian, similar to (1), whose minimum encodes the optimal solution of the given problem, see [14]. This means that the minimum can only be achieved when an optimal spin configuration (ground state) is found, where the latter corresponds to the solution of the problem. However, even when an adequate Hamiltonian description of a problem is found, mapping the problem onto the coupling coefficients within $\boldsymbol{J}$ and $\boldsymbol{h}$ is not always straightforward. To address this problem, we propose a mathematical framework, which directly yields the coupling coefficients in case the Hamiltonian of the considered problem is given.

In previous work [21], we have proposed a real-time-capable algorithm for emulating an oscillator-based Ising machine that can solve optimization problems with no Zeeman term. The algorithm is based on the wave digital concept, which is a powerful tool for emulating the behavior of electrical circuits. In particular, this concept is known for its numerical robustness and massive parallelism when it comes to emulating large electrical networks [22]. In this work, we aim to present a generalization of the circuit, on which the algorithm is based, that also considers the Zeeman term. To explain the functionality and robustness of the proposed algorithm, we recapitulate the stability analysis presented in [4], which is based on Lyapunov's stability theory. Here, we propose a modified Lyapunov function that now fulfills the properties of a strict Lyapunov function, as opposed to the one found in literature [4]. Furthermore, we provide a novel concept for finding out when an oscillator-based Ising machine has solved a mapped problem besides convergency. This concept serves as both an explanation and a numerical proof of the Ising machine's functionality.

The remainder of this paper is structured as follows: Section 2 gives some preliminary remarks on the nomenclature used throughout this work. In section 3 we introduce a framework for mapping optimization problems onto the Ising machine. Section 4 deals with the functionality, stability, and modeling of a phase-oscillator-based Ising machine. In section 5, we show emulation results to validate the discussions of the previous section. Finally, section 6 summarizes our contributions and gives a brief outlook on future research in the context of this work.

2 | PRELIMINARIES

A graph $\mathcal{G} = (\mathcal{V}, \mathcal{E})$ consists of $|\mathcal{V}| = n$ vertices and $|\mathcal{E}| = m$ edges. Two vertices μ and ν are said to be adjacent if the edge set $\mathcal{E}$ contains a corresponding edge denoted by $(\mu, \nu) \in \mathcal{E}$. In most cases, the edges are undirected, i.e. when $(\mu, \nu) \in \mathcal{E}$, then this indirectly implies $(\nu, \mu) \in \mathcal{E}$, unless the problem is explicitly declared to have directed edges. The matrix $\boldsymbol{A}$ denotes the adjacency matrix of the graph, which is always symmetric $\boldsymbol{A} = \boldsymbol{A}^{\mathrm{T}}$ and contains zeros on its main diagonal, as we do not consider any form of self loops. The matrix $\bar{\boldsymbol{A}}$ denotes the co-adjacency matrix of the graph and is given by:

$$\bar{\boldsymbol{A}} = \mathbb{1}_n \mathbb{1}_n^{\mathrm{T}} - \boldsymbol{1} - \boldsymbol{A} \,. \tag{2}$$

This matrix is always symmetric $\bar{\boldsymbol{A}} = \bar{\boldsymbol{A}}^{\mathrm{T}}$ and contains zeros on its main diagonal. Lastly, a complete graph is a graph, where a path exists from every vertex to every other vertex in the graph. A set of vertices (or oscillators) are said to be completely coupled/connected, if their graph representation constitutes a complete graph.

3 | PROBLEM MAPPING

Mapping an optimization problem to an oscillator-based Ising machine first requires formulating the problem as a Quadratic Unconstrained Binary Optimization problem (QUBO):

$$\min_{\boldsymbol{x}} \left\{ \boldsymbol{x}^{\mathrm{T}} \boldsymbol{Q} \boldsymbol{x} \right\} \,, \quad x_\nu \in \{0, 1\} \,. \tag{3}$$

Here, we refer to $\boldsymbol{x}$ as a vector of bit variables and $\boldsymbol{Q} \in \mathbb{R}^{n \times n}$ as the coefficient matrix, which encodes the optimization problem. The problem of minimizing the Ising Hamiltonian is essentially a QUBO, since it can always be stated as

$$\min_{\boldsymbol{s}} \{ H \} \,, \quad \text{with} \quad H = -\boldsymbol{s}_{\mathrm{e}}^{\mathrm{T}} \boldsymbol{J}_{\mathrm{e}} \boldsymbol{s}_{\mathrm{e}} \,, \quad \boldsymbol{J}_{\mathrm{e}} = \begin{bmatrix} \boldsymbol{J} & \frac{\boldsymbol{h}}{2} \\ \frac{\boldsymbol{h}^{\mathrm{T}}}{2} & 0 \end{bmatrix} \,, \quad \text{and} \quad \boldsymbol{s}_{\mathrm{e}} = \begin{bmatrix} \boldsymbol{s} \\ 1 \end{bmatrix} \,, \tag{4}$$

where $\boldsymbol{s}_\mathrm{e}$ is an extended vector of spin variables and $\boldsymbol{J}_\mathrm{e}$ is an extended coefficient matrix, which now also encodes the Zeeman term. In the following, we refer to the problem of minimizing the Hamiltonian defined in (4) as an Ising problem. Note, the relation between the two variables $\boldsymbol{x}$ and $\boldsymbol{s}$ is bijective:

$$\boldsymbol{x} = \frac{1}{2}[\boldsymbol{s} + \mathbb{1}] \quad \Longleftrightarrow \quad \boldsymbol{s} = 2\boldsymbol{x} - \mathbb{1}\,. \tag{5}$$

Therefore, every QUBO can be reformulated as an Ising problem and vice versa.

To give an example of problem mapping, we consider the maximum cut problem (max-cut), arguably the most popular problem in association with the Ising machine. This is partly due to the direct correspondence of the optimization problem with the Ising model. Given a weighted graph $\mathcal{G} = (\mathcal{V}, \mathcal{E})$ with the weighted adjacency matrix $\boldsymbol{W}$, the maximum cut problem asks for a partitioning of the graph's vertices into two complementary sets, such that the number of edges between the sets is maximal,

$$\max_{\boldsymbol{s}} \{\mathrm{cut}\{\boldsymbol{s}\}\} = \min_{\boldsymbol{s}} \left\{\boldsymbol{s}^\mathrm{T}\boldsymbol{W}\boldsymbol{s}\right\}\,, \qquad \text{with} \qquad \mathrm{cut}\{\boldsymbol{s}\} = \frac{1}{4}\sum_{\mu=1}^{n}\sum_{\nu=1}^{n} w_{\mu\nu}[1 - s_\mu s_\nu] = \frac{1}{4}\left[\mathbb{1}^\mathrm{T}\boldsymbol{W}\mathbb{1} - \boldsymbol{s}^\mathrm{T}\boldsymbol{W}\boldsymbol{s}\right]. \tag{6}$$

Evidently, the coupling coefficients in (1) are determined by:

$$\boldsymbol{J} = -\boldsymbol{W} \quad \text{and} \quad \boldsymbol{h} = \boldsymbol{0}\,. \tag{7}$$

One spin variable sometimes do not suffice for representing local decisions, which have more than two possible outcomes. In this case, a common approach is to use multiple spin variables. Thus, we obtain subsets of spin variables, which are mutually coupled to encode the considered problem. For that reason, it can be beneficial to represent the spin variables in the form of a matrix, whose columns each represent a subset of spin variables:

$$\boldsymbol{S} = \left[\boldsymbol{s}_1,\, \boldsymbol{s}_2,\, \ldots,\, \boldsymbol{s}_m\right]\,, \quad \text{with} \quad \boldsymbol{S} \in \mathbb{R}^{k\times m}\,, \quad mk = n\,, \quad \text{and} \quad \boldsymbol{s} = \mathrm{vec}(\boldsymbol{S})\,. \tag{8}$$

Here, m is the number of subsets, k is the number of spin variables in each subset, while $\mathrm{vec}(\boldsymbol{S})$ denotes the vectorization of the matrix $\boldsymbol{S}$. Equivalent to (6), we define a matrix of bit variables:

$$\boldsymbol{X} = \frac{1}{2}[\boldsymbol{S} + \mathbb{1}\mathbb{1}^\mathrm{T}]\,, \quad \text{with} \quad \boldsymbol{x} = \mathrm{vec}(\boldsymbol{X})\,. \tag{9}$$

Throughout this manuscript, we will show that the Hamiltonian representation of many graph-related tasks can be formulated as

$$H = H_\ell + \sum_{\lambda=0}^{\ell-1} H_\lambda\,, \quad \text{with} \quad H_\lambda = \mathrm{tr}\left(\boldsymbol{Q}_\lambda^\mathrm{T}\boldsymbol{S}^\mathrm{T}\boldsymbol{R}_\lambda\boldsymbol{S}\right) \quad \text{and} \quad H_\ell = \boldsymbol{q}_\ell^\mathrm{T}\boldsymbol{S}^\mathrm{T}\boldsymbol{r}_\ell\,, \tag{10}$$

where $\boldsymbol{Q}_\lambda \in \mathbb{R}^{m\times m}$ and $\boldsymbol{R}_\lambda \in \mathbb{R}^{k\times k}$ are real matrices (usually adjacency matrices), $\boldsymbol{q}_\ell \in \mathbb{R}^k$ and $r_\ell \in \mathbb{R}^m$ are real vectors, and $\mathrm{tr}(\cdot)$ denotes the trace operator. The relationship between (10) and the canonical formulation of the Ising Hamiltonian (1) is given by:

$$H = \sum_{\lambda=1}^{\ell} H_\lambda\,, \quad \text{with} \quad H_\lambda = \boldsymbol{s}^\mathrm{T}[\boldsymbol{Q}_\lambda \otimes \boldsymbol{R}_\lambda]\boldsymbol{s} \quad \text{and} \quad H_\ell = [\boldsymbol{q}_\ell \otimes \boldsymbol{r}_\ell]^\mathrm{T}\boldsymbol{s}\,, \tag{11}$$

where $\otimes$ denotes the Kronecker product. A thorough derivation of this relationship is given in the appendix. Now, we would like to give a graph-theoretical interpretation of this mapping scheme, so we rewrite the partitioned Hamiltonians as a linear combination of bilinear forms:

$$H_\lambda = \sum_{\mu=0}^{m} q_{\lambda,\mu\mu}\boldsymbol{s}_\mu^\mathrm{T}\boldsymbol{R}_\lambda\boldsymbol{s}_\mu + \sum_{\mu\neq\nu}^{m} q_{\lambda,\mu\nu}\boldsymbol{s}_\mu^\mathrm{T}\boldsymbol{R}_\lambda\boldsymbol{s}_\nu\,, \quad \text{with} \quad q_{\lambda,\mu\nu} = \boldsymbol{e}_\mu^\mathrm{T}\boldsymbol{Q}_\lambda\boldsymbol{e}_\nu\,. \tag{12}$$

The first sum maps m topologically identical disjoint subgraphs onto the Ising Hamiltonian. Their interconnections are described by $\boldsymbol{R}_\lambda$, where the edge weights of the μ-th subgraph are uniformly scaled by the factor $q_{\mu\mu}$. The second sum maps the interconnection between the vertices of the μ-th and ν-th subgraph. Again, the interconnections and their weights are described by the adjacency matrix $\boldsymbol{R}_\lambda$ and are uniformly scaled by the factor $q_{\mu\nu}$. By comparing the coefficients of (1) with (11), we obtain the following relationship between both representations:

$$\boldsymbol{J} = -\sum_{\mu=0}^{\ell-1}[\boldsymbol{Q}_\lambda \otimes \boldsymbol{R}_\lambda] \quad \text{and} \quad \boldsymbol{h} = -[\boldsymbol{q}_\ell \otimes \boldsymbol{r}_\ell]\,. \tag{13}$$

Figure 1 Left: An arbitrary spin configuration for an Ising lattice. Right: Compact representation of an Ising machine with the same configuration as the left side. The appearing oscillators assume a relative phase shift of either 0 or π. A relative phase shift of π is interpreted as "spin up" (blue), while a relative phase shift of 0 is interpreted as "spin down" (red).

To map an Ising problem to the Ising machine, we must encode the coupling coefficients into the couplings of the oscillators. Fig. 1 depicts the solution of an Ising problem with four coupling coefficients $J_{\mu\nu}$. Here, the coefficients have been mapped onto the conductances of the Ising machine depicted on the right side. The following sections give a systematic derivation of the coupling coefficients from the underlying QUBO formulation. Here, we will deal with different kinds of optimization problems (including NP-problems), where each problem will introduce a new type of cost function or constraint. The problems are hierarchically organized by the difficulty of their QUBO formulation. The purpose of this analysis is to obtain a reservoir of different cost functions and constraints, whose mapping onto the Ising machine should be the simplified by our contribution. The resulting formalism is especially useful for systematically mapping densely constrained problems onto the Ising machine. In particular, we would like to draw the reader's attention to the recurring vector-valued representations, which appear in many graph-based optimization problems. These terms usually appear as multiple sums over node or edge subsets in the original QUBO formulations, see [14] for an overview. Such a representation makes it very difficult to discern the coupling structure and the associated weights. However, this interpretation becomes very simple and intuitive, when the suggested formalism is applied.

3.1 | Binary Integer Linear Programming

Binary Integer Linear Programming (BILP) is an optimization task that asks us to maximize a linear cost function subject to a set of linear equality constraints [23]:

$$\max_{\boldsymbol{x}} \boldsymbol{d}^{\mathrm{T}}\boldsymbol{x}\,, \quad \text{s. t.} \quad \boldsymbol{W}\boldsymbol{x} = \boldsymbol{b}\,. \tag{14a}$$

The entries of the vector $\boldsymbol{d} \in \mathbb{R}^n$ scale the bit variables according to their importance or impact. The entries of $\boldsymbol{W} \in \mathbb{R}^{k\times n}$ are the coefficients of the considered linear constraints, while $\boldsymbol{b}$ contains the constant equality constraints. The QUBO formulation associated with this problem reads [14],

$$H = H_0 + H_1\,, \quad H_0 = -c_0\,\boldsymbol{d}^{\mathrm{T}}\boldsymbol{x}\,, \quad H_1 = c_1\|\boldsymbol{b} - \boldsymbol{W}\boldsymbol{x}\|^2\,, \tag{14b}$$

where $\|\cdot\|$ denotes the Euclidian norm. The coefficients c_ν weigh the different parts of the Hamiltonian according to their importance. In some Ising problems, certain choices of these coefficients are beneficial for enhancing the performance of the Ising machine [14]. Now, since we have no subsets of bit variables, the corresponding Hamiltonian of the Ising problem can be directly obtained by applying (5):

$$H = \underbrace{\frac{c_1}{4}\boldsymbol{s}^{\mathrm{T}}\boldsymbol{W}^{\mathrm{T}}\boldsymbol{W}\boldsymbol{s}}_{\text{mutual coupling}} + \underbrace{\frac{c_1}{2}\left[\mathbb{1}^{\mathrm{T}}\boldsymbol{W}^{\mathrm{T}}\boldsymbol{W} - 2\boldsymbol{b}^{\mathrm{T}}\boldsymbol{W} - \frac{c_0}{c_1}\boldsymbol{d}^{\mathrm{T}}\right]\boldsymbol{s}}_{\text{Zeeman term}} \underbrace{- c_1\left[\boldsymbol{b}^{\mathrm{T}}\boldsymbol{b} - \boldsymbol{b}^{\mathrm{T}}\boldsymbol{W}\mathbb{1} + \mathbb{1}^{\mathrm{T}}\boldsymbol{W}^{\mathrm{T}}\boldsymbol{W}\mathbb{1} - \frac{c_0}{2c_1}\boldsymbol{d}^{\mathrm{T}}\mathbb{1}\right]}_{\text{offset}}\,. \tag{14c}$$

Comparing the coefficients of (14c) with (1) then yields the desired coupling coefficients:

$$\boldsymbol{J} = -\frac{c_1}{4}\boldsymbol{W}^{\mathrm{T}}\boldsymbol{W} \quad \text{and} \quad \boldsymbol{h} = -\frac{c_1}{2}\left[\boldsymbol{W}^{\mathrm{T}}\boldsymbol{W}\mathbb{1} - 2\boldsymbol{W}^{\mathrm{T}}\boldsymbol{b} - \frac{c_0}{c_1}\boldsymbol{d}\right]. \tag{14d}$$

The offset appearing in (14c) is not important w.r.t. the coupling coefficients. However, it ensures that the minimum of the Hamiltonian, corresponding to the solution of the problem, stays at zero.

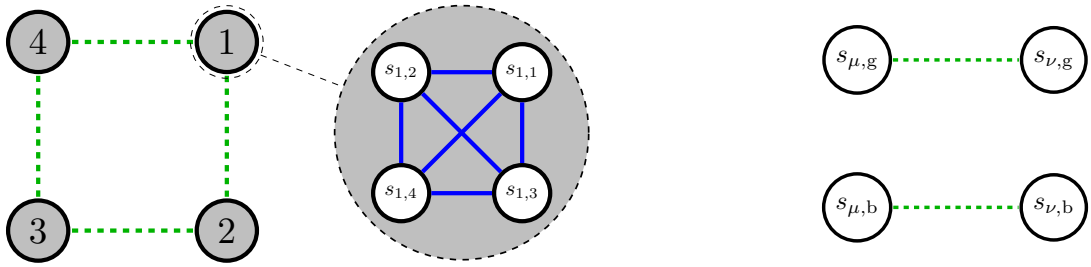

Figure 2 An example of a graph with $m = 4$ and $k = 4$. Every vertex in the compact graph is a condensed representation of a complete graph with $k = 4$ vertices. The vertices of the latter are the spin variables representing the color of the corresponding vertex. An explicit representation of the green dashed edges is given on the right side of the figure.

3.2 | Minimal Vertex Cover

Given an undirected graph $\mathcal{G} = (\mathcal{V}, \mathcal{E})$ with m vertices and p edges, a vertex cover is a set of vertices covering all edges, i.e. every edge is incident to a vertex in the set. The minimal vertex cover problem asks for the minimal number of vertices that must be colored in order to obtain a vertex cover[24]:

$$\min_{\boldsymbol{x}} \ \mathbb{1}^{\mathrm{T}}\boldsymbol{x}\,, \quad \text{s. t.} \quad x_\mu + x_\nu \geq 1 \quad \text{for all} \quad (\mu,\nu) \in \mathcal{E}\,. \tag{15a}$$

Here, the validity of the vertex cover is embedded into the inequality constraint. The QUBO formulation of this problem reads[14]:

$$H = H_0 + H_1\,, \quad H_0 = c_0 \mathbb{1}^{\mathrm{T}}\boldsymbol{x}\,, \quad H_1 = \frac{c_1}{2}[\mathbb{1} - \boldsymbol{x}]^{\mathrm{T}}\boldsymbol{A}[\mathbb{1} - \boldsymbol{x}]\,, \tag{15b}$$

with the adjacency matrix $\boldsymbol{A}$ of $\mathcal{G}$. Again, no subsets of bit variables appear in this problem. Applying (5) yields

$$H = \underbrace{\frac{c_1}{8}\boldsymbol{s}^{\mathrm{T}}\boldsymbol{A}\boldsymbol{s}}_{\text{mutual coupling}} \underbrace{- \mathbb{1}^{\mathrm{T}}\left[\frac{c_1}{4}\boldsymbol{A} - \frac{c_0}{2}\mathbf{1}\right]\boldsymbol{s}}_{\text{Zeeman term}} + \underbrace{\frac{c_1}{4}p + \frac{c_0}{2}m}_{\text{offset}}\,. \tag{15c}$$

The desired coefficients are given by:

$$\boldsymbol{J} = -\frac{c_1}{8}\boldsymbol{A} \quad \text{and} \quad \boldsymbol{h} = \left[\frac{c_1}{4}\boldsymbol{A} - \frac{c_0}{2}\mathbf{1}\right]\mathbb{1}\,. \tag{15d}$$

3.3 | Graph Coloring

Given an undirected graph $\mathcal{G} = (\mathcal{V}, \mathcal{E})$ with m vertices and p edges, the graph coloring problem asks us to color the graph with k colors such that two adjacent vertices never share the same color. Here, we have two conditions that must be fulfilled: every vertex must have exactly one color and two adjacent vertices should not have the same color. Considering that every color can only be represented by one binary variable, we must introduce k binary variables for the different colors of each vertex. We can then formulate the optimization problem as follows:

$$\min_{\boldsymbol{x}} \ 1\,, \quad \text{s. t.} \quad \sum_{\varkappa=1}^{k} x_{\nu,\varkappa} = 1\,, \qquad x_{\mu,\varkappa} + x_{\nu,\varkappa} \leq 1\,, \qquad x_{\nu,\varkappa} \in \{0,1\}\,. \tag{16a}$$

A possible QUBO formulation reads[14]

$$H = H_1 + H_2\,, \quad \text{with} \quad H_1 = \left\|\boldsymbol{X}^{\mathrm{T}}\mathbb{1} - \mathbb{1}\right\|^2\,, \quad H_2 = \frac{1}{2}\operatorname{tr}(\boldsymbol{A}\boldsymbol{X}^{\mathrm{T}}\boldsymbol{X})\,, \quad \text{and} \quad \boldsymbol{X} \in \mathbb{R}^{m\times k}\,, \tag{16b}$$

where $\boldsymbol{A}$ denotes the adjacency matrix of $\mathcal{G}$. Every column of $\boldsymbol{X}$ contains k bit variables $x_{\nu,\varkappa}$ for each possible color of the ν-th vertex. To obtain the equivalent Ising problem, we apply (9), which yields the Hamiltonian

$$H = \underbrace{\frac{1}{4}\operatorname{tr}(\boldsymbol{S}^{\mathrm{T}}\mathbb{1}\mathbb{1}^{\mathrm{T}}\boldsymbol{S}) + \frac{1}{8}\operatorname{tr}(\boldsymbol{A}\boldsymbol{S}^{\mathrm{T}}\boldsymbol{S})}_{\text{mutual coupling}} + \underbrace{\frac{1}{4}\mathbb{1}^{\mathrm{T}}\left[\boldsymbol{A} + [2k-4]\mathbf{1}\right]\boldsymbol{S}^{\mathrm{T}}\mathbb{1}}_{\text{Zeeman term}} + \underbrace{\frac{1}{4}\left[pk + n[k-2]^2\right]}_{\text{offset}}\,. \tag{16c}$$

From (13), we can deduce the desired coupling coefficients:

$$\boldsymbol{J} = -\frac{1}{4}[\mathbf{1} \otimes \mathbb{1}\mathbb{1}^{\mathrm{T}}] - \frac{1}{8}[\boldsymbol{A} \otimes \mathbf{1}] \quad \text{and} \quad \boldsymbol{h} = -\frac{1}{4}\left[[\boldsymbol{A} + [2k-4]\mathbf{1}]\,\mathbb{1} \otimes \mathbb{1}\right] . \tag{16d}$$

A graphical illustration of the coupling scheme is given Fig. 2.

3.4 | Hamiltonian Cycle

Given a directed or undirected graph $\mathcal{G} = (\mathcal{V}, \mathcal{E})$ with m vertices and p edges, can one find a cycle that visits every vertex exactly once? Essentially, a Hamiltonian cycle imposes two conditions: every vertex must be visited exactly once and only adjacent vertices are visitable from the current vertex. To formulate this problem as a binary optimization problem, one can introduce m bit variables representing the current positioning in the graph for every graph traversal. However, this implies that we must add the condition that the current position must always be unique. Overall, we can formulate the problem as follows:

$$\min_{\boldsymbol{x}} \; 1 \qquad \text{s. t.} \qquad \sum_{\mu=1}^{n} x_{\mu,\nu} = 1\,, \qquad \sum_{\nu=1}^{n} x_{\mu,\nu} = 1\,, \qquad x_{\mu,\lambda} + x_{\nu,\lambda+1} = 0\,, \qquad \text{for all} \qquad (\mu,\nu) \notin \mathcal{E}\,. \tag{17a}$$

The corresponding QUBO formulation then reads [14]

$$\begin{aligned} &H = H_1 + H_2 + H_3\,, \qquad H_1 = c_1 \|\boldsymbol{X}\mathbb{1} - \mathbb{1}\|^2\,, \quad H_2 = c_1 \left\|\boldsymbol{X}^{\mathrm{T}}\mathbb{1} - \mathbb{1}\right\|^2\,, \\ &H_3 = c_1 \operatorname{tr}(\bar{\boldsymbol{A}}\boldsymbol{X}^{\mathrm{T}}\boldsymbol{P}^{\mathrm{T}}\boldsymbol{X})\,, \quad \boldsymbol{P} = \begin{bmatrix} \mathbf{0}^{\mathrm{T}} & 1 \\ \mathbf{1} & \mathbf{0} \end{bmatrix}\,, \qquad \boldsymbol{X} \in \mathbb{R}^{n\times n}\,, \end{aligned} \tag{17b}$$

where $\bar{\boldsymbol{A}}$ is the co-adjacency matrix defined in (2) and where every column of $\boldsymbol{X}$ represents a subset of bit variables. After applying the bijective mapping relation (9), we obtain the Hamiltonian of the Ising problem:

$$H = \underbrace{\frac{c_1}{4}\left[\operatorname{tr}(\mathbb{1}\mathbb{1}^{\mathrm{T}}\boldsymbol{S}^{\mathrm{T}}\boldsymbol{S}) + \operatorname{tr}(\boldsymbol{S}^{\mathrm{T}}\mathbb{1}\mathbb{1}^{\mathrm{T}}\boldsymbol{S}) + \operatorname{tr}(\bar{\boldsymbol{A}}\boldsymbol{S}^{\mathrm{T}}\boldsymbol{P}^{\mathrm{T}}\boldsymbol{S})\right]}_{\text{mutual coupling}} + \underbrace{\frac{c_1}{2}\mathbb{1}^{\mathrm{T}}\left[\bar{\boldsymbol{A}} + [2m-4]\mathbf{1}\right]\boldsymbol{S}^{\mathrm{T}}\mathbb{1}}_{\text{Zeeman term}} + \underbrace{\frac{mc_1}{4}[2[m-2]^2 + m^2 - m - p]}_{\text{offset}}\,. \tag{17c}$$

The desired coupling coefficients are given by:

$$\boldsymbol{J} = -\frac{c_1}{4}\left[\mathbb{1}\mathbb{1}^{\mathrm{T}} \otimes \mathbf{1} + \mathbf{1} \otimes \mathbb{1}\mathbb{1}^{\mathrm{T}} + \bar{\boldsymbol{A}} \otimes \boldsymbol{P}^{\mathrm{T}}\right] \quad \text{and} \quad \boldsymbol{h} = -\frac{c_1}{2}\left[\left[\bar{\boldsymbol{A}} + [2m-4]\mathbf{1}\right]\mathbb{1} \otimes \mathbb{1}\right] . \tag{17d}$$

A graphical illustration of the coupling scheme is given in Fig. 3.

3.5 | Traveling Salesman Problem

Let $\mathcal{G} = (\mathcal{V}, \mathcal{E})$ be a directed or undirected weighted graph with m vertices and the weighted adjacency matrix $\boldsymbol{W}$, where each edge (μ, ν) is associated with the weight $w_{\mu\nu}$ representing a distance between two cities. Can one find a Hamiltonian cycle such that the distance covered while traveling through the cycle is minimal? The optimization task is the same as (17a) except that we now have a non-constant cost function:

$$\min_{\boldsymbol{x}} \sum_{(\mu,\nu)\in\mathcal{E}} w_{\mu\nu}\, x_{\mu\nu} \qquad \text{s. t.} \qquad \sum_{\mu=1}^{n} x_{\mu,\nu} = 1\,, \qquad \sum_{\nu=1}^{n} x_{\mu,\nu} = 1\,, \qquad x_{\mu,\lambda} + x_{\nu,\lambda+1} = 0\,, \qquad \text{for all} \qquad (\mu,\nu) \notin \mathcal{E}\,. \tag{18a}$$

Extending the Ising formulation of the Hamiltonian cycle problem to cover the traveling salesman problem is achieved by adding the following term to (17b),

$$H_0 = c_0 \operatorname{tr}(\boldsymbol{W}\boldsymbol{X}^{\mathrm{T}}\boldsymbol{P}^{\mathrm{T}}\boldsymbol{X})\,. \tag{18b}$$

This ensures the minimum of the Hamiltonian is given by a variable configuration that provides the shortest Hamiltonian cycle. In order to avoid violating the conditions of a Hamiltonian cycle, the constant coefficient c_2 must be chosen to be in the interval $0 < c_0 < c_1/\max(w_{\mu\nu})$ [14]. Now, apply (9) to obtain:

$$\frac{4}{c_0}H_0 = \underbrace{\operatorname{tr}(\boldsymbol{W}\boldsymbol{S}^{\mathrm{T}}\boldsymbol{P}^{\mathrm{T}}\boldsymbol{S})}_{\text{mutual coupling}} + \underbrace{2\mathbb{1}^{\mathrm{T}}\boldsymbol{W}\boldsymbol{S}^{\mathrm{T}}\mathbb{1}}_{\text{Zeeman term}} + \underbrace{m\mathbb{1}^{\mathrm{T}}\boldsymbol{W}\mathbb{1}}_{\text{offset}}\,. \tag{18c}$$

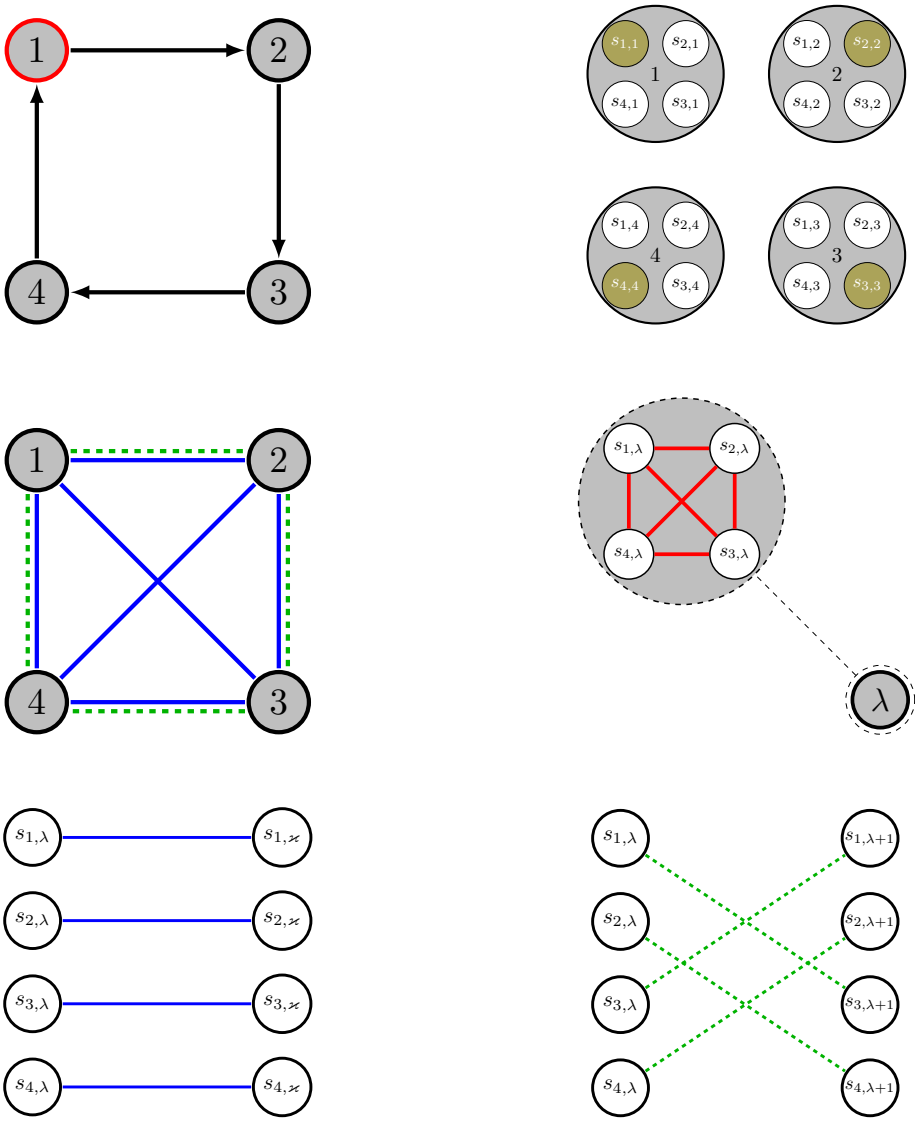

Figure 3 Top left: Trivial instance and solution of the Hamiltonian cycle problem with the starting point 1. Here, the edge labels represent the order of the transitions. Top Right: Illustration of the solution of in terms of spin variable subsets. The highlighted variables represent the current positioning after each graph traversal. Center left: Compact representation of the coupling scheme. Center right: Every node in contains four variables with an all to all coupling. Bottom left: Explicit illustration of the blue couplings. Bottom right: Explicit representation of the green couplings.

Finally, the desired coupling coefficients are finally given by:

$$\boldsymbol{J} = -\frac{1}{4}\left[[c_0\boldsymbol{W} + c_1\bar{\boldsymbol{A}}] \otimes \boldsymbol{P}^{\mathrm{T}}\right] - \frac{c_1}{4}\left[\mathbb{1}\mathbb{1}^{\mathrm{T}} \otimes \mathbf{1} + \mathbf{1} \otimes \mathbb{1}\mathbb{1}^{\mathrm{T}}\right] \quad \text{and} \quad \boldsymbol{h} = -\frac{c_1}{2}\left[\left[\bar{\boldsymbol{A}} + \frac{c_0}{c_1}\boldsymbol{W} + [2m-4]\mathbf{1}\right]\mathbb{1} \otimes \mathbb{1}\right]. \tag{18d}$$

A graphical illustration of the resulting coupling is presented in Fig. 4.

To conclude this section, we have provided a systematic procedure for mapping QUBO formulations from literature onto the coupling coefficients of an Ising problem. In principle, we argue that almost any graph-related task is formulated as a linear combination of the terms that have appeared in the discussed problems. In fact, even problems that are not necessarily graph-related can be interpreted this way. For example, problems with images, such as image restoration[25], can be interpreted as a

Figure 4 Compact representation of the coupling scheme for the traveling salesman problem. The blue and green couplings are the same as in Fig. 3. The magenta coupling is explicitly illustrated on the right side of the figure.

lattice of vertices with nearest-neighbor interaction. By calculating the associated adjacency matrix, one can easily map the problem onto our suggested formalism and obtain the coupling coefficients. Thus, we have bridged the gap between the QUBO formulation and the coupling coefficients needed for mapping a problem onto the Ising machine. For the sake of convenience, the essential relations are summarized in table 1 of the appendix.

4 | AN ISING MACHINE BASED ON PHASE OSCILLATORS

Now that we have addressed the systematic mapping of optimization problems oscillator-based Ising machines, we can discuss the reasons, which qualify oscillator networks to function as Ising machines. The general idea is to let a diffusively coupled oscillator network emulate the behavior of coupled spins, whose energy is described by the Ising Hamiltonian. If the Ising Hamiltonian is somehow mapped onto the energy of the electrical system, then we expect the free-running system to find a state configuration that minimizes its energy and consequently the mapped Hamiltonian. However, this requires the oscillators to act like the spins from the Ising model. Therefore, every oscillator is subjected to a special type of forcing, so-called subharmonic injection locking (SHIL), which enforces bi-stable phase behavior in the stationary state[26], i.e. a phase shift of 0 or π with respect to some reference oscillation. To explain the functionality of the considered circuit in a formal but intuitive manner, we approximate the circuit's dynamics by phase reduction[27]. This results in a phase model, similar to the Kuramoto model[28], which captures the phase behavior of the original circuit through a system of differential equations:

$$\dot{\varphi}_\mu = \Delta\omega_\mu + k_\mathrm{c}\,\omega_{\mathrm{c}_\mu} - k_\mathrm{s}\,\omega_{\mathrm{s}_\mu}\,, \tag{19a}$$

$$\Delta\omega_\mu = [\omega_\mu - \omega_0]\,, \tag{19b}$$

$$\omega_{\mathrm{c}_\mu} = \omega_0 \sum_{\nu=1}^{n} J_{\mu\nu}\,\Im\left\{e^{\mathrm{j}[\varphi_\nu-\varphi_\mu]}\right\}\,, \tag{19c}$$

$$\omega_{\mathrm{s}_\mu} = \omega_0 \Im\left\{e^{\mathrm{j}2\varphi_\mu}\right\}\,. \tag{19d}$$

Here, φ_μ denotes the phase shift of the μ-th oscillator. The constant $\Delta\omega_\mu$ represents the difference between the frequency of the μ-th oscillator ω_μ and the network's central frequency ω_0. The subfunction ω_{c_μ} represents the inter-oscillator coupling between the μ-th oscillator and the remainder of the network, with the bias coupling strength k_c and the couplings weights $J_{\mu\nu}$. Similarly, ω_{s_μ} represents the SHIL coupling of the μ-th oscillator with the coupling strength k_s. For a detailed derivation of the phase model, we refer the interested reader to[4].

4.1 | Stability Analysis

The functionality of the phase-oscillator-based Ising machine can be understood by analyzing the stability of the system. The considered phase model, in particular, is a special case, where this stability analysis is relatively simple, due to it being a gradient system. The trajectories of the said system always follow the steepest descent of an associated scalar potential function[29], which leads to asymptotic stability in the sense of Lyapunov. A sufficient condition for the existence of a potential function is the symmetry of the Jacobian associated with the vector field of the considered system[30]. In the following, we derive an analytical

expression for the Jacobian and show it to be indeed symmetric. To that end, we first rewrite (19) as

$$\Sigma : \begin{cases} \dot{\varphi} & = \Delta\omega + k_\mathrm{c}\,\omega_\mathrm{c}(\varphi) - k_\mathrm{s}\,\omega_\mathrm{s}(\varphi) \\ \Delta\omega & = \omega - \omega_0\,\mathbb{1} \\ \omega_\mathrm{c}(\varphi) & = \omega_0 \mathfrak{T}\left\{\mathbf{diag}(\boldsymbol{s}^\mathrm{H})\,\boldsymbol{J}\,\boldsymbol{s}\right\} \\ \omega_\mathrm{s}(\varphi) & = \omega_0 \mathfrak{T}\left\{\mathbf{diag}(\boldsymbol{s})\boldsymbol{s}\right\} \end{cases}, \tag{20}$$

where $\Delta\omega = [\Delta\omega_1, \Delta\omega_2, \ldots, \Delta\omega_n]^\mathrm{T}$, $\varphi = [\varphi_1, \varphi_2, ..., \varphi_n]^\mathrm{T}$. Furthermore, we introduce the vector $\boldsymbol{s}(\varphi) = e^{\mathrm{j}\varphi}$, which projects the phase values φ_μ onto continuous spin values $s_\mu \in [-1, 1]$, which can be interpreted like the spin variables of the Ising Hamiltonian. In general, the partial derivatives of the phase equation only consist of two types of elements:

$$\frac{\partial\dot{\varphi}_\mu}{\partial\varphi_\varkappa} = \omega_0 k_\mathrm{c} \begin{cases} -e_\varkappa^\mathrm{T}\mathfrak{R}\left\{\mathbf{diag}(\boldsymbol{s}^\mathrm{H})\,\boldsymbol{J}\boldsymbol{s}\right\}, & \varkappa = \mu \\ J_{\varkappa,\mu}\mathfrak{R}\left\{s_\varkappa\, s_\mu^*\right\}, & \varkappa \neq \mu. \end{cases}. \tag{21}$$

Consequently, the Jacobian in analytical form can be given by:

$$\boldsymbol{J}_f(\varphi) = k_\mathrm{c}\,\boldsymbol{J}_{f_\mathrm{c}}(\varphi) - k_\mathrm{s}\,\boldsymbol{J}_{f_\mathrm{s}}(\varphi)\,, \qquad \text{with} \tag{22a}$$

$$\boldsymbol{J}_{f_\mathrm{c}}(\varphi) = \boldsymbol{\Omega}_1(\varphi) - \mathbf{diag}(\boldsymbol{\Omega}_1(\varphi)\mathbb{1})\,, \tag{22b}$$

$$\boldsymbol{J}_{f_\mathrm{s}}(\varphi) = 2\omega_0\mathfrak{R}\left\{\mathbf{diag}(\boldsymbol{s})^2\right\}, \qquad \text{and} \tag{22c}$$

$$\boldsymbol{\Omega}_1(\varphi) = \omega_0\mathfrak{R}\left\{\mathbf{diag}(\boldsymbol{s}^\mathrm{H})\,\boldsymbol{J}\;\mathbf{diag}(\boldsymbol{s})\right\}. \tag{22d}$$

Here, $\boldsymbol{J}_{f_\mathrm{c}}(\varphi)$ is a Hermitian matrix containing the partial derivatives of ω_c, whereas $\boldsymbol{J}_{f_\mathrm{s}}(\varphi)$ is a real diagonal matrix containing the partial derivatives of ω_s. Hence, the Jacobian $\boldsymbol{J}_f$, as a linear combination, is also Hermitian. Therefore, the considered network has a scalar potential function $V(\varphi)$, which can be obtained by integrating the state equation with respect φ and choosing the integration constant such that the negative gradient of $V(\varphi)$ coincides with the state equation,

$$\nabla_\varphi V(\varphi) = -\dot{\varphi}\,, \tag{23a}$$

with

$$V(\varphi) = -\Delta\omega^\mathrm{T}\varphi + k_\mathrm{c}V_\mathrm{c}(\varphi) - k_\mathrm{s}V_\mathrm{s}(\varphi)\,, \tag{23b}$$

$$V_\mathrm{c}(\varphi) = \frac{\omega_0}{2}\left[\mathbb{1}^\mathrm{T}\boldsymbol{J}\mathbb{1} - \mathfrak{R}\left\{\boldsymbol{s}^\mathrm{H}\boldsymbol{J}\boldsymbol{s}\right\}\right], \tag{23c}$$

$$V_\mathrm{s}(\varphi) = \frac{\omega_0}{2}\left[\mathfrak{R}\left\{\boldsymbol{s}^\mathrm{T}\boldsymbol{s}\right\} - n\right]. \tag{23d}$$

The function $V(\varphi)$ is a Lyapunov function candidate that must be modified, so it remains a potential function but fulfills the conditions of a strict Lyapunov function. We refer the interested to[31] for an overview on the properties and applications of Lyapunov functions. Now, it can be verified that $V(\varphi)$ fulfills two of the three conditions of a strict Lyapunov function. The third condition requires a valid Lyapunov function to be positive semidefinite. Up to this point, $V(\varphi)$ is only positive definite if the coupling coefficients $J_{\mu\nu}$ are non-negative, which generally does not hold. To construct a strict Lyapunov function, we suggest applying a simple rectification:

$$V(\varphi) = -\Delta\omega^\mathrm{T}\varphi + k_\mathrm{c}V_\mathrm{c}(\varphi) - k_\mathrm{s}V_\mathrm{s}(\varphi) \tag{24a}$$

$$V_\mathrm{c}(\varphi) = \frac{\omega_0}{2}\left[\mathbb{1}^\mathrm{T}\boldsymbol{J}_+\mathbb{1} - \mathfrak{R}\left\{\boldsymbol{s}^\mathrm{H}\boldsymbol{J}\boldsymbol{s}\right\}\right], \tag{24b}$$

$$V_\mathrm{s}(\varphi) = \frac{\omega_0}{2}\left[\mathfrak{R}\left\{\boldsymbol{s}^\mathrm{T}\boldsymbol{s}\right\} - n\right]. \tag{24c}$$

The entries of $\boldsymbol{J}_+$ are the absolute values of the entries of $\boldsymbol{J}$. This change ensures the potential function stays positive, when the coupling coefficients are negative without having any effects on its gradient. Equation (24) now fulfills all the properties of a strict Lyapunov function as opposed to the Lyapunov function appearing in literature[4]. The asymptotic stability of the network can be inferred from examining the time derivative of its Lyapunov function:

$$\dot{V}(\varphi) = \left[\nabla_\varphi V(\varphi)\right]^\mathrm{T}\dot{\varphi} = -\left\|\nabla_\varphi V(\varphi)\right\|^2 < 0\,. \tag{25}$$

Here, we make use of (23) to obtain the last equality. The application of a SHIL-signal forces the oscillators to assume the values $\varphi_\mu \in \{0, \pi\}$ in the stationary state, such that we have $\mathfrak{R}\left\{\boldsymbol{s}^\mathrm{T}\boldsymbol{s}\right\} = n$ and $\mathfrak{R}\left\{\boldsymbol{s}^\mathrm{H}\boldsymbol{J}\boldsymbol{s}\right\} = \boldsymbol{s}^\mathrm{T}\boldsymbol{J}\boldsymbol{s}$. Thus, the Lyapunov function can

be rewritten as

$$V(\varphi) = -\boldsymbol{s}^{\mathrm{T}}\boldsymbol{J}\boldsymbol{s} + c(\varphi)\,, \qquad \text{with} \qquad c(\varphi) = -\Delta\boldsymbol{\omega}^{\mathrm{T}}\boldsymbol{\varphi} + \mathbb{1}^{\mathrm{T}}\boldsymbol{J}_{+}\,\mathbb{1} \tag{26}$$

where $c(\varphi)$ (asymptotically) represents a constant offset. The Lyapunov function coincides with the Ising Hamiltonian up to a constant offset. Equation (25) shows that the network minimizes the derived Lyapunov function and therefore also naturally minimizes the Ising Hamiltonian, which explains its functionality as an Ising machine.

4.2 | Electrical Model

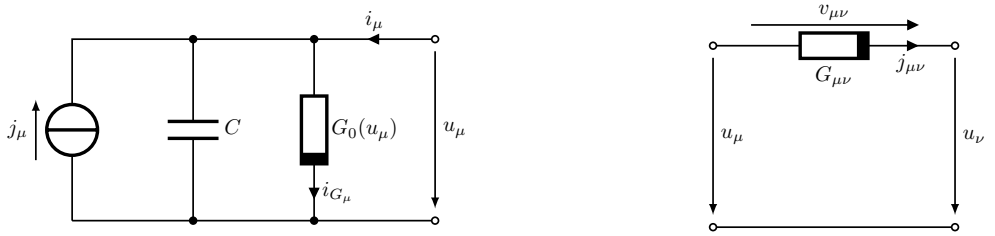

Figure 5 Left: Equivalent circuit of the phase oscillator. Right: Electrical coupling element representing the phase coupling in the modified Kuramoto model.

In this section, we synthesize an electrical circuit for the considered phase model. This circuit is used for two purposes: to emulate the behavior of the circuit and to extend the underlying model, so it incorporates the Zeeman term. To this end, we apply an equivalency transformation to (19), where we associate the phase φ_μ with a scaled voltage quantity $\pi\hat{u}/u_\mu$ resulting in,

$$\pi\frac{\dot{u}_\mu}{\hat{u}} = \Delta\omega_\mu + k_{\mathrm{c}}\,\omega_{\mathrm{c}_\mu} - k_{\mathrm{s}}\,\omega_{\mathrm{s}_\mu}\,, \tag{27a}$$

$$\omega_{\mathrm{c}_\mu} = \omega_0 \sum_{\nu=1}^{n} J_{\mu\nu}\sin\left(\pi\frac{u_\nu - u_\mu}{\hat{u}}\right)\,, \tag{27b}$$

$$\omega_{\mathrm{s}_\mu} = \omega_0 \sin\left(2\pi\frac{u_\mu}{\hat{u}}\right)\,, \tag{27c}$$

with the voltage normalization constant $\hat{u} = 1\,\mathrm{V}$. Now, consider the circuit on the left of Fig. 5, which is governed by:

$$\dot{u}_\mu = \frac{1}{C}\left[j_\mu - i_{G_\mu} + i_\mu\right]\,. \tag{28}$$

Equation (28) is now used to model the dynamics of (27). Since ω_{c_μ} represents an inter-oscillator interaction, it is associated with the external coupling current i_μ. The term ω_{s_μ} accounts for the SHIL-signal, which induces a self-coupling term in (19) and is therefore associated with the current i_{G_μ}. Finally, the residual current j_μ is associated with the frequency degeneration $\Delta\omega_\mu$ resulting in:

$$j_\mu = 2\hat{u}f_0 C\Delta\omega_\mu\,, \qquad \omega_0 = 2\pi f_0\,, \tag{29a}$$

$$i_{G_\mu} = I_{\mathrm{s}}\sin\left(2\pi\frac{u_\mu}{\hat{u}}\right)\,, \qquad I_{\mathrm{s}} = 2\hat{u}f_0 C k_{\mathrm{s}}\,, \tag{29b}$$

$$i_\mu = I_{\mathrm{c}}\sum_{\nu=1}^{n} J_{\mu\nu}\sin\left(\pi\frac{u_\nu - u_\mu}{\hat{u}}\right)\,, \qquad I_{\mathrm{c}} = 2\hat{u}f_0 C k_{\mathrm{c}}\,. \tag{29c}$$

We can now use Ohm's law to obtain an expression for the nonlinear conductance:

$$i_{G_\mu} = G_0(u_\mu)\,u_\mu\,, \quad \text{with} \quad G_0(u_\mu) = G_{\mathrm{s}}\,2\pi\,\mathrm{si}\left(2\pi\frac{u_\mu}{\hat{u}}\right) \quad \text{and} \quad G_{\mathrm{s}} = \frac{I_G}{\hat{u}} = 2f_0 C k_{\mathrm{s}}\,. \tag{30}$$

The external coupling currents model the inter-oscillator coupling of the original oscillator network. Considering that each phase oscillator (left side of Fig. 5) is a reduced representative of an actual oscillator, we see that the topology of the original network is retained in the circuit of the phase model. Thus, the currents i_μ results from coupling multiple phase oscillators via

a diffusive coupling network, as depicted in Fig. 6 on the example of four coupled phase oscillators. The coupling elements are given by nonlinear conductors (right side of Fig. 5), because they implement the nonlinear coupling of the phase model. The conductances can, again, be determined by first writing out the particular Ohmic relation:

$$j_{\mu\nu} = G_{\mu\nu}\, v_{\mu\nu} = G_{\mu\nu}\,[u_\mu - u_\nu]\,. \tag{31}$$

Here, the orientation of the currents $j_{\mu\nu}$ is chosen, so they originate from phase oscillator with lower indices and flow towards phase oscillators with higher indices, see Fig. 6. This simplifies the description of the current flow and enables using Kirchhoff's current law to obtain the relationship:

$$j_{\mu\nu} = I_\mathrm{c}\, J_{\mu\nu} \sin\left(\pi \frac{u_\mu - u_\nu}{\hat{u}}\right)\,. \tag{32}$$

With equations (31) and (32), the coupling conductances can be formulated as

$$G_{\mu\nu} = G_\mathrm{c} J_{\mu\nu}\, \pi\, \mathrm{si}\left(\pi \frac{u_\mu - u_\nu}{\hat{u}}\right)\,, \quad \text{with} \quad G_\mathrm{c} = \frac{I_\mathrm{c}}{\hat{u}} = 2 f_0 C k_\mathrm{c}\,, \tag{33}$$

where $\mathrm{si}(0) = 1$, otherwise $\mathrm{si}(x) = \sin(x)/x$.

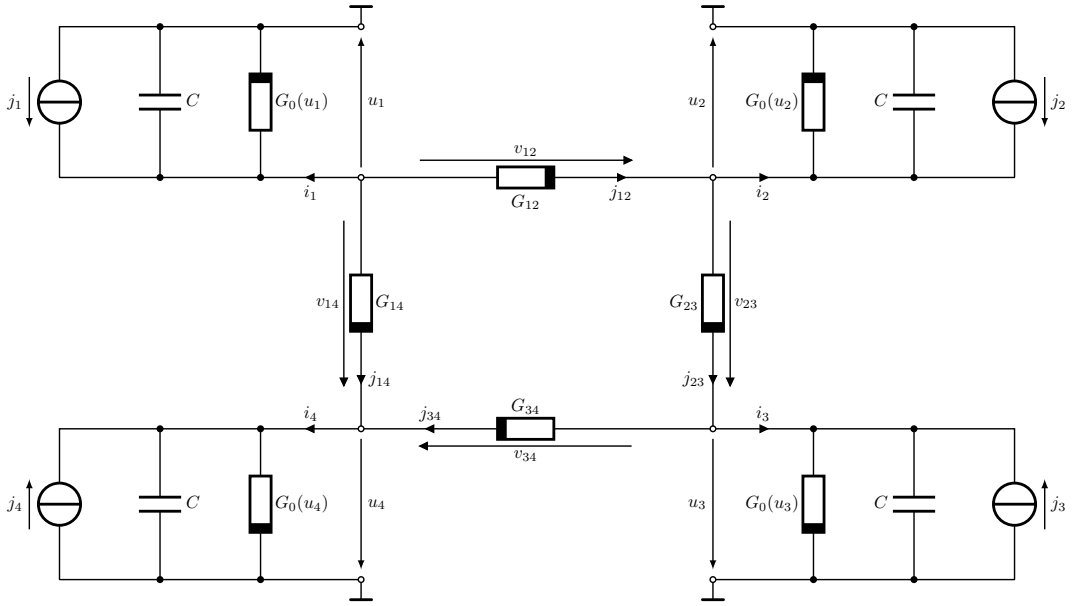

Figure 6 Four coupled phase oscillators.

Note, the coupling of the original oscillator network, whose behavior is described by the phase model, is linear. This statement is based on the fact that the coupling coefficients $J_{\mu\nu}$ are constant.

4.3 | Implementing the Zeeman Term

Up to this point, the electrical model does not support incorporating the Zeeman term. However, this term appears in many Ising formulations and should therefore be considered. The equivalent formulation of the Ising Hamiltonian in (4) reveals a possible realization of the Zeeman term, where all oscillators are coupled to a reference oscillator with a locked phase value of $s_{n+1} = +1$. The Zeeman term coefficients, given by $J_{\mu[n+1]} = h_\mu/2$, are then incorporated into the conductances coupling the phase oscillators to the reference oscillator:

$$G_{\mu[n+1]}(u) = G_\mathrm{c} \frac{h_\mu}{2}\, \pi\, \mathrm{si}\left(\pi \frac{u}{\hat{u}}\right)\,. \tag{34}$$

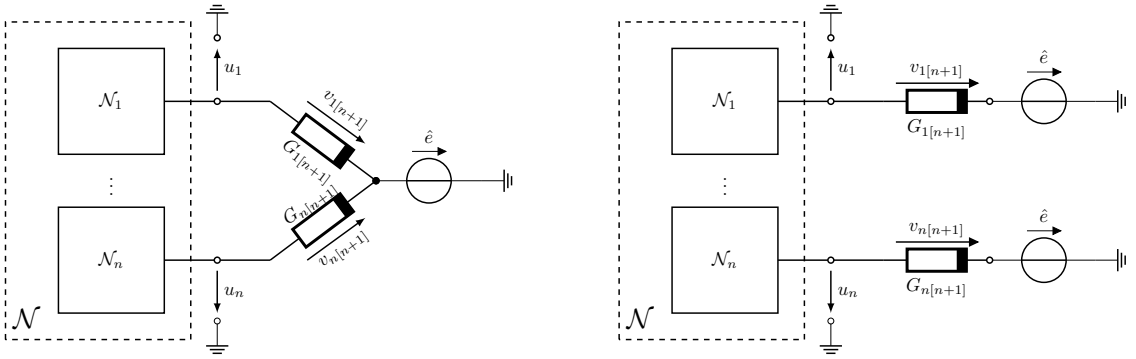

Figure 7 Left: General topology of n interconnected oscillators $\mathcal{N}$ coupled to a reference signal in order to account for the Zeeman term. Right: Equivalent electrical circuit of the circuit depicted on the left.

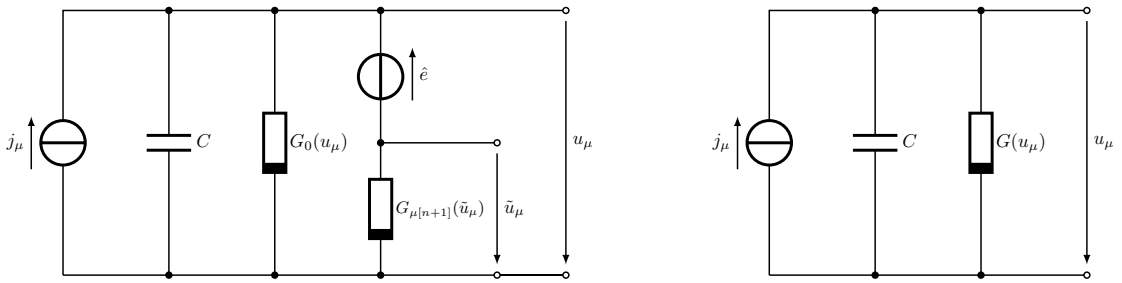

Figure 8 Left: The reference source and the parallel conductors connected to it are inserted into the oscillator circuit. Right: Omitting the voltage source by redefining the nonlinearity of the conductor.

Practically, it is a very simple approach that comes with one drawback. Simulations of the Ising machine using this approach show that the reference oscillator can break out of its locked state. In such situations, the phase evolution of the Ising machine is distorted, which usually results in an invalid or suboptimal solution. A much more reliable approach is to make use of an ideal voltage source supplying the reference signal, see the left of Fig. 7. To decouple the circuit, we can split it at the node of the voltage source into n resistive voltage sources, see the right side of Fig. 7. Then, every resistive voltage source can be combined with the corresponding oscillator circuit, see the left of Fig. 8. To omit the voltage source, we can simply redefine $G_{\mu[n+1]}$ as:

$$G_{\mu[n+1]}(u) = G_\mathrm{c}\frac{h_\mu}{2}\,\pi\,\mathrm{si}\left(\pi\frac{u-\hat{e}}{\hat{u}}\right), \quad \text{with} \quad \hat{e} = 1\mathrm{V}\,. \tag{35}$$

Now, we have two parallel conductors, which can be simplified to one conductor with the conductance:

$$G(u) = G_\mathrm{s}\,2\pi\,\mathrm{si}\left(2\pi\frac{u}{\hat{u}}\right) + G_\mathrm{c}\frac{h_\mu}{2}\,\pi\,\mathrm{si}\left(\pi\frac{u-\hat{e}}{\hat{u}}\right)\,. \tag{36}$$

These equivalent transformations allow reusing the same circuit as the one presented on the left side of Fig. 5, but with a different internal conductance $G(u)$, see the right side of Fig. 8.

5 | EMULATION RESULTS AND DISCUSSION

Now that we have derived an electrical circuit for the considered phase model, we now discuss briefly discuss our preferred method of emulation. Here, we make use of the wave digital concept[32], which is a powerful tool for emulating the behavior of large electrical networks in a highly parallel fashion. In previous work[21], we have discussed how efficient wave digital models can be derived for the considered phase model. The electrical model of this work presents an extension of our past results, because it now also implements the Zeeman term. However, the electrical model is structurally identical, which allows exploiting the same methods discussed in[21] to emulate the phase-oscillator-based Ising machine.

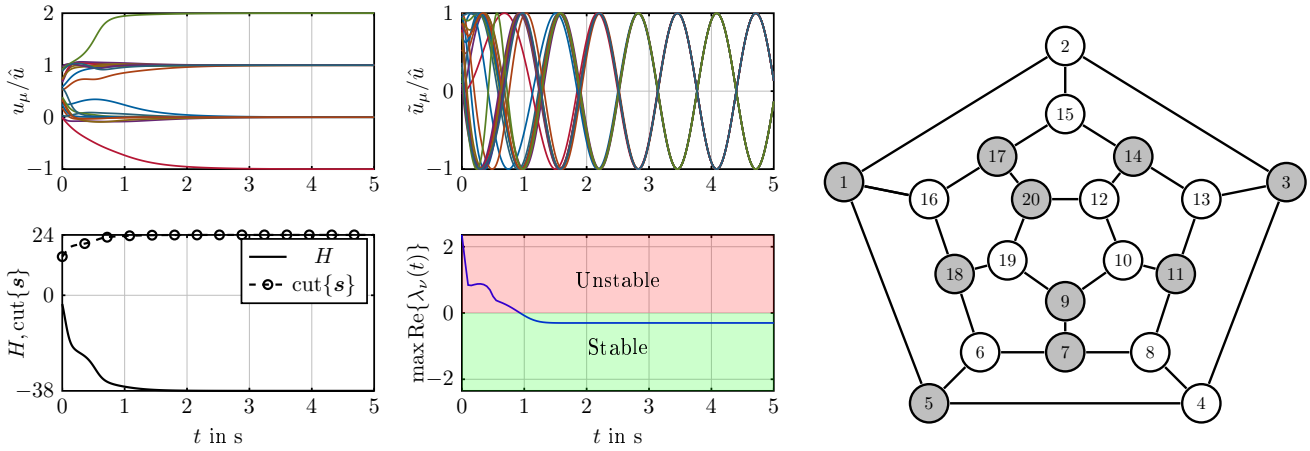

Figure 9 Top left: Normalized voltage outputs of the Ising machine's oscillators. Top center: Reconstructed output oscillations corresponding to the normalized output voltages. Bottom left: Value of the Ising Hamiltonian and the cut size over time. Bottom center: Real part of the minimal and maximal eigenvalues of the linearized system over time. Right: Benchmark graph including the solution of the Ising machine.

To test the Ising machine on one practical example, we solve a max-cut problem with a graph from [33] that is known to have a cut size of 24, see the right side of Fig. 9. The emulation parameters used for the electrical circuit are given in table 1. Furthermore, the machine is started at some random initial states in the interval $[0, 1]$ V.

Emulation parameters	
$\omega_0 = 5 \cdot 10^9$ rad/s	$k_\mathrm{c} = 0.5$
$C = 1$ nF	$k_\mathrm{s} = 0.4$

Table 1 Emulation parameters for the maximum cut problem.

The machine partitions the graph into the two subgraphs, as denoted by the gray and white vertices on the left side of Fig. 9. This partitioning can be interpreted from the output voltages of the oscillators u_μ on the top left of Fig. 9. The central top figure shows the oscillations of the original network, which have been reconstructed using the relationship

$$\tilde{u}_\mu = \hat{u} \sin(\omega_0 t + \varphi_\mu)\,, \quad \text{with} \quad \hat{u} = 1\mathrm{V}\,. \tag{37}$$

Overall, the machine evolves, so it minimizes the Ising Hamiltonian, which can be seen on the bottom right side of Fig. 9. Since the problem of minimizing the cut size has been mapped to the Hamiltonian (using the coefficients in (7)), the cut size is maximized when the Hamiltonian is minimized. The correlation between the stability and functionality can be clearly seen on the central bottom figure of Fig. 9. Here, we calculated the eigenvalues of the Jacobian (22) and plotted the eigenvalue with the maximal real part. All other eigenvalues are not plotted, but lie beneath the drawn one. The plot implies that some eigenvalues initially have a positive real part, but eventually evolve to have a negative real part once the machine finds the optimal solution. In other words, the optimal solution of the given task has been mapped onto a stable equilibrium of the system. This is, for the first time, a numerical proof of stability, which relates to previous analysis [4,8] but has yet to be conducted. Furthermore, it has another important implication, which we now would like to discuss: when the machine is turned on, it is not possible to know when it has solved the problem. However, if all eigenvalues have a negative real part, then this implies that the system trajectories have entered a local attractor with a stable equilibrium. Once the system enters this attractor, the machine is not able to exit the attractor's domain (unless externally perturbed), which implies that the machine has solved the problem. Otherwise, it is only possible to presume that the machine is done when it exhibits some convergency behavior, which is not necessarily true. In principle, one could argue that it is possible to decode the solution after 1 s in this example.

6 | CONCLUSION AND OUTLOOK

Overall, this work is intended to give a broad overview on oscillator-based Ising machines. In the first part, we have discussed the mapping of optimization problems onto an oscillator-based Ising machine. To simplify this process, we have proposed a mathematical framework which aids in mapping quadratic unconstrained optimization problems onto the couplings of an Ising machine. Here, we reviewed four representative optimization problems with different cost functions and constraint types to give an overview on how quadratic unconstrained optimization problems can generally be mapped onto an Ising machine. This analysis has shown that many problems can indeed be systematically mapped by an appropriate grouping of the decision variables.

In the second part of this work, we recapitulated the concept of a phase-oscillator-based Ising machine. Here, we gave a generalization of our previous work by synthesizing an ideal circuit that also considers the linear term appearing in the Ising Hamiltonian, the so-called Zeeman term. In combination with the wave digital concept, this circuit can be used as an algorithm for simulated annealing. To explain the functionality and robustness of the proposed algorithm, we have conducted a thorough stability analysis. The results of this analysis have been numerically verified on a practical example, where we have discussed the effects of problem mapping on the phase space of the phase-oscillator-based Ising machine. In a future work, we hope to find a systematic mapping procedure of general binary optimization problems onto an oscillator-based Ising machine.

ACKNOWLEDGMENTS

This work was funded by the Deutsche Forschungsgemeinschaft (DFG, German Research Foundation) – Project-ID 434434223 – SFB 1461 and DFG-404291403.

Conflict of interest

The authors declare no potential conflict of interests.

How to cite this article: B. Al Beattie and K. Ochs (2022), Primer on Ising Formulations for Oscillator-Based Ising Machines, *Int. J. Numer. Model., 2021;00:1–6.*

APPENDIX

Sum Terms in QUBO Formulation	Representation within Framework	Coupling Coefficient Matrix $\boldsymbol{J}$
$\left[\sum_{\nu=1}^{n} s_\nu\right]^2$	$\mathrm{tr}(\boldsymbol{s}\boldsymbol{s}^\mathrm{T}) = \|\boldsymbol{s}\|^2 = \boldsymbol{s}^\mathrm{T}\boldsymbol{s}$	$\boldsymbol{J} = -\boldsymbol{1}$
$\sum_{\mu=1}^{n}\left[\sum_{\nu=1}^{n} w_{\mu\nu}s_\nu\right]^2$	$\mathrm{tr}(\boldsymbol{W}^\mathrm{T}\boldsymbol{W}\boldsymbol{s}\boldsymbol{s}^\mathrm{T}) = \|\boldsymbol{W}\boldsymbol{s}\|^2 = \boldsymbol{s}^\mathrm{T}\boldsymbol{W}^\mathrm{T}\boldsymbol{W}\boldsymbol{s}$	$\boldsymbol{J} = -\boldsymbol{W}^\mathrm{T}\boldsymbol{W}$
$\sum_{(\mu,\nu)\in\mathcal{E}} s_\mu s_\nu$	$\mathrm{tr}(\boldsymbol{A}\boldsymbol{s}\boldsymbol{s}^\mathrm{T}) = \boldsymbol{s}^\mathrm{T}\boldsymbol{A}\boldsymbol{s}$	$\boldsymbol{J} = -\boldsymbol{A}$
$\sum_{\nu=1}^{n}\left[\sum_{\varkappa=1}^{k} s_{\nu,\varkappa}\right]^2$	$\mathrm{tr}(\boldsymbol{S}^\mathrm{T}\mathbb{1}\mathbb{1}^\mathrm{T}\boldsymbol{S}) = \left\|\boldsymbol{S}^\mathrm{T}\mathbb{1}\right\|^2$	$\boldsymbol{J} = -\boldsymbol{1}\otimes\mathbb{1}\mathbb{1}^\mathrm{T}$
$\sum_{\varkappa=1}^{k}\left[\sum_{\nu=1}^{n} s_{\nu,\varkappa}\right]^2$	$\mathrm{tr}(\mathbb{1}\mathbb{1}^\mathrm{T}\boldsymbol{S}^\mathrm{T}\boldsymbol{S}) = \|\boldsymbol{S}\mathbb{1}\|^2$	$\boldsymbol{J} = -\mathbb{1}\mathbb{1}^\mathrm{T}\otimes\boldsymbol{1}$
$\sum_{\varkappa=1}^{k}\sum_{(\mu,\nu)\in\mathcal{E}} s_{\mu,\varkappa}s_{\nu,\varkappa}$	$\mathrm{tr}(\boldsymbol{A}\boldsymbol{S}^\mathrm{T}\boldsymbol{S})$	$\boldsymbol{J} = -\boldsymbol{A}\otimes\boldsymbol{1}$
$\sum_{\varkappa=1}^{k}\sum_{(\mu,\nu)\in\mathcal{E}} w_{\mu\nu}s_{\mu,\varkappa}s_{\nu,\varkappa+1}$	$\mathrm{tr}(\boldsymbol{W}\boldsymbol{S}^\mathrm{T}\boldsymbol{P}^\mathrm{T}\boldsymbol{S})$	$\boldsymbol{J} = -\boldsymbol{W}\otimes\boldsymbol{P}^\mathrm{T}$
$\sum_{\varkappa=1}^{k}\sum_{(\mu,\nu)\notin\mathcal{E}} s_{\mu,\varkappa}s_{\nu,\varkappa+1}$	$\mathrm{tr}(\bar{\boldsymbol{A}}\boldsymbol{S}^\mathrm{T}\boldsymbol{P}^\mathrm{T}\boldsymbol{S})$	$\boldsymbol{J} = -\bar{\boldsymbol{A}}\otimes\boldsymbol{P}^\mathrm{T}$

Table 1 Mapping between the sum terms from QUBO formulations and terms of the suggested framework.

In the following we show how the relationship between (1) and (10) is derived. Here, we make use of the trace operator equalities,

$$\mathrm{tr}(\boldsymbol{M}\boldsymbol{N}\boldsymbol{O}) = \mathrm{tr}(\boldsymbol{O}\boldsymbol{M}\boldsymbol{N}) = \mathrm{tr}(\boldsymbol{N}\boldsymbol{O}\boldsymbol{M})\,, \quad \mathrm{tr}(\boldsymbol{M}^\mathrm{T}\boldsymbol{N}) = \mathrm{vec}(\boldsymbol{M})^\mathrm{T}\mathrm{vec}(\boldsymbol{N})\,, \tag{1}$$

and the Kronecker product formula,

$$\boldsymbol{M}\boldsymbol{N}\boldsymbol{O} = \boldsymbol{P} \quad \Longleftrightarrow \quad [\boldsymbol{O}^\mathrm{T}\otimes\boldsymbol{M}]\mathrm{vec}(\boldsymbol{N}) = \mathrm{vec}(\boldsymbol{P})\,, \tag{2}$$

where all appearing matrices are real and squared. Applying these equalities to every H_λ allows for rewriting (10) as:

$$H = \sum_{\lambda=1}^{\ell} H_\lambda\,, \quad \text{with} \quad H_\lambda = \boldsymbol{s}^\mathrm{T}[\boldsymbol{Q}_\lambda\otimes\boldsymbol{R}_\lambda]\boldsymbol{s} \quad \text{and} \quad H_\ell = [\boldsymbol{q}_\ell\otimes\boldsymbol{r}_\ell]^\mathrm{T}\boldsymbol{s}\,. \tag{3}$$

References

1. Yang YS, Kim Y. Recent Trend of Neuromorphic Computing Hardware: Intel's Neuromorphic System Perspective. *2020 International SoC Design Conference (ISOCC)* 2020: 218-219. doi: 10.1109/ISOCC50952.2020.9332961

2. Nowshin F, Zhang Y, Liu L, Yi Y. Recent Advances in Reservoir Computing With A Focus on Electronic Reservoirs. *2020 11th International Green and Sustainable Computing Workshops (IGSC)* 2020: 1-8. doi: 10.1109/IGSC51522.2020.9290858

3. Kalinin KP, Berloff NG. Computational complexity continuum within Ising formulation of NP problems. *Communications Physics* 2022; 5(1): 20. doi: 10.1038/s42005-021-00792-0

4. Wang T, Roychowdhury J. OIM: Oscillator-Based Ising Machines for Solving Combinatorial Optimisation Problems. *Unconventional Computation and Natural Computation* 2019: 232-256.

5. Chou J, Bramhavar S, Ghosh S, Herzog W. Analog Coupled Oscillator Based Weighted Ising Machine. *Scientific Reports* 2019; 9(1): 14786. doi: 10.1038/s41598-019-49699-5

6. Afoakwa R, Zhang Y, Vengalam UKR, Ignjatovic Z, Huang M. BRIM: Bistable Resistively-Coupled Ising Machine. *2021 IEEE International Symposium on High-Performance Computer Architecture (HPCA)* 2021: 749-760. doi: 10.1109/HPCA51647.2021.00068

7. Vaidya J, Surya Kanthi RS, Shukla N. Creating electronic oscillator-based Ising machines without external injection locking. *Scientific Reports* 2022; 12(1): 981. doi: 10.1038/s41598-021-04057-2

8. Dutta S, Khanna A, Datta S. Understanding the Continuous-Time Dynamics of Phase-Transition Nano-Oscillator-Based Ising Hamiltonian Solver. *IEEE Journal on Exploratory Solid-State Computational Devices and Circuits* 2020; 6(2): 155-163. doi: 10.1109/JXCDC.2020.3045074

9. Takesue H, Inagaki T, Inaba K, Honjo T. Solving large-scale optimization problems with coherent Ising machine. *2017 Conference on Lasers and Electro-Optics Pacific Rim (CLEO-PR)* 2017: 1-2. doi: 10.1109/CLEOPR.2017.8118781

10. Pierangeli D, Marcucci G, Conti C. Large-Scale Ising Machine Based on Spatial Light Modulation. *2019 Conference on Lasers and Electro-Optics Europe and European Quantum Electronics Conference (CLEO/Europe-EQEC)* 2019: 1-1. doi: 10.1109/CLEOE-EQEC.2019.8872368

11. Böhm F, Verschaffelt G, Sande V. dG. A Compact and Inexpensive Coherent Ising Machine Based on Opto-Electronic Feedback for Solving Combinatorial Optimization Problems. *2020 Conference on Lasers and Electro-Optics (CLEO)* 2020: 1-2.

12. Reifenstein S, Kako S, Khoyratee F, Leleu T, Yamamoto Y. Coherent Ising Machines with Optical Error Correction Circuits. *Advanced Quantum Technologies* 2021; 4(11): 2100077. doi: https://doi.org/10.1002/qute.202100077

13. Ising E. Beitrag zur Theorie des Ferromagnetismus. *Zeitschrift für Physik* 1925; 31(1): 253-258. doi: 10.1007/BF02980577

14. Lucas A. Ising formulations of many NP problems. *Frontiers in Physics* 2014; 2. doi: 10.3389/fphy.2014.00005

15. Matsumoto N, Hamakawa Y, Tatsumura K, Kudo K. Distance-based clustering using QUBO formulations. *Scientific Reports* 2022; 12(1): 2669. doi: 10.1038/s41598-022-06559-z

16. Mahasinghe A, Fernando V, Samarawickrama P. QUBO formulations of three NP problems. *Journal of Information and Optimization Sciences* 2021; 42(7): 1625-1648. doi: 10.1080/02522667.2021.1930657

17. Takabatake K, Yanagisawa K, Akiyama Y. Solving Generalized Polyomino Puzzles Using the Ising Model. *Entropy* 2022; 24: 354. doi: 10.3390/e24030354

18. Singh AK, Jamieson K, McMahon PL, Venturelli D. Dynamics and Regularization for Near-Optimal MIMO Detection. *IEEE Transactions on Wireless Communications* 2022: 1-1. doi: 10.1109/TWC.2022.3189604

19. Yoshimura N, Tawada M, Tanaka S, et al. Efficient Ising Model Mapping for Induced Subgraph Isomorphism Problems Using Ising Machines. *2019 IEEE 9th International Conference on Consumer Electronics (ICCE-Berlin)* 2019: 227-232. doi: 10.1109/ICCE-Berlin47944.2019.8966218

20. Kanamaru S, Kawamura K, Tanaka S, et al. Mapping Constrained Slot-Placement Problems to Ising Models and its Evaluations by an Ising Machine. *2019 IEEE 9th International Conference on Consumer Electronics (ICCE-Berlin)* 2019: 221-226. doi: 10.1109/ICCE-Berlin47944.2019.8966207

21. Ochs K, Al Beattie B, Jenderny S. An Ising Machine Solving Max-Cut Problems based on the Circuit Synthesis of the Phase Dynamics of a Modified Kuramoto Model. *2021 IEEE International Midwest Symposium on Circuits and Systems (MWSCAS)* 2021: 982-985. doi: 10.1109/MWSCAS47672.2021.9531734

22. Fettweis A. Robust Numerical Integration Using Wave-Digital Concepts. *Multidimensional Systems and Signal Processing* 2006; 17(1): 7-25. doi: 10.1007/s11045-005-6236-3

23. Williams HP. *Logic and Integer Programming*. Springer Publishing Company, Incorporated. 1st ed. 2009.

24. Vazirani V. *Approximation Algorithms*. Springer Berlin Heidelberg . 2002.

25. Keuchel J, Schnorr C, Schellewald C, Cremers D. Binary partitioning, perceptual grouping, and restoration with semidefinite programming. *IEEE Transactions on Pattern Analysis and Machine Intelligence* 2003; 25(11): 1364-1379. doi: 10.1109/TPAMI.2003.1240111

26. Neogy A, Roychowdhury J. Analysis and design of sub-harmonically injection locked oscillators. 2012. doi: 10.1109/DATE.2012.6176677

27. Nakao H. Phase reduction approach to synchronisation of nonlinear oscillators. *Contemporary Physics* 2016; 57(2): 188-214. doi: 10.1080/00107514.2015.1094987

28. Kuramoto Y. Self-entrainment of a population of coupled non-linear oscillators. *International Symposium on Mathematical Problems in Theoretical Physics* 1975: 420–422.

29. Howse JW, Abdallah CT, Heileman GL. Gradient and Hamiltonian Dynamics Applied to Learning in Neural Networks. In: ; 1995.

30. Schultz DG, Gibson JE. The variable gradient method for generating liapunov functions. *Transactions of the American Institute of Electrical Engineers, Part II: Applications and Industry* 1962; 81(4): 203–210.

31. Lakshmikantham V, Matrosov V, Sivasundaram S. *Vector Lyapunov Functions and Stability Analysis of Nonlinear Systems*. Mathematics and Its ApplicationsSpringer Netherlands . 1991.

32. Fettweis A. Wave digital filters: Theory and practice. *Proceedings of the IEEE* 1986; 74(2): 270-327. doi: 10.1109/PROC.1986.13458

33. Cook SA. An Overview of Computational Complexity. *Commun. ACM* 1983; 26(6): 400–408. doi: 10.1145/358141.358144

AUTHOR BIOGRAPHY

Bakr Al Beattie. was born in Bagdad, Irak, in 1998. He received his B.Sc. degree in Information Technology and his M.Sc. degree in Automatic Control from the Ruhr-University Bochum (RUB) in 2020 and 2022, respectively. Since 2021 he is with the Chair of Digital Communications Systems at the Department of Electrical Engineering and Information Technology at Ruhr-University Bochum to pursue his Ph.D. degree. He is also involved as a member of the collaborative research center (CRC) 1461, entitled ”Neurotronics”, which is working on the development of neuromorphic computation technology. His research interests include software emulation with the wave digital concept, neuromorphic technology, memristive circuits, bio-inspired computing, and self-organizing circuits.

Karlheinz Ochs. was born in Lingen, Germany in 1968. He received the Diploma and the Dr.-Ing. degree in Electrical Engineering from the University of Paderborn, Germany, in 1996 and 2001, respectively. He habilitated in 2011 with his thesis “Theory of time-variant linear transmission systems” at the Ruhr University Bochum, Germany, where he is currently a senior researcher. His representative work includes wave digital emulation of linear and nonlinear systems, memristive neuromorphic circuits, numerical integration methods, and time-variant communication systems. Since 2010 he is working in the field of memristive device for neuromorphic circuits especially as a principal investigator for the DFG (German Research Society) Research Group FOR2093 entitled: “Memristive Devices for neuronal Systems”. Furthermore, he is also involved as a principal investigator of the collaborative research center (CRC) 1461, entitled ”Neurotronics”, where his research is focused on the wave digital emulation of bio-inspired self-organizing memristively coupled oscillator networks.